# 利用自製奈米壓印機來進行奈米結構製程的研究

學生：劉子漢　　　　　　　　　　　指導教授：孫建文教授

國立交通大學
應用化學系碩士班

## 摘要

奈米科學與奈米科技的發展仰賴於製造技術的提升與改進。近十年來，隨著半導體微影技術的進步。人們已經可以很順利地製造尺寸小於 100nm 的微型結構及元件。然而，當奈米結構的尺寸小於 22nm 時，製造過程會變的很複雜及困難。奈米壓印技術是一種次世代微影技術。此種技術利用轉印的方式可以將模板上的奈米圖形轉印至基板上。奈米壓印技術不僅可以製造奈米結構，也可以用來進行大範圍面積的轉印。因此，奈米壓印技術是下世代微影技術中最具潛力的一種微影技術。

本實驗室自行設計一台熱壓、紫外線固化兩用式奈米壓印機台。我們利用電子束微影技術製作出適用的壓印模子並利用此機台來進行奈米結構的製造。此外，我們還進行 fracture induced structuring (FIS)的製程研究。希望能利用此機台及壓印技術來大量、快速、便宜地製造具有奈米結構的樣品。

# Development of nanoimprint techniques and their applications with a home-made nanoimprintor

Student：Zih Han Liou                    Advisor：Dr. Kien Wen Sun

Institute of Applied Chemistry
National Chiao Tung University

## Abstract

The development of nanoscience and nanotechnology depends strongly on the capabilities of the fabrication techniques that are used for patterning and chemically modifying materials at the nanoscale. The spectacular progress in this field has been successfully demonstated by the conventional lithography in the past decade. While the difficulty becomes more clearly when the feature size of the patterns are made even smaller (down to sub-45 nm). Nanoimprint lithography is one of the next generation lithography and this technology is promising and has the potential for the duplication of nano-scale and large-area patterns.

In our investigation , we built up a home-made nanoimprintor and designed the e-beam patterned molds. We have demonstrated the sub-200 nm H-NIL、UV-NIL results with this facility. Other than that , we also carried out experiments on the fracture induced structuring (FIS) process and manufactured uniform nanogratings with an easy and fast manner.

# Table of Contents

## Chapter 1 Introduction

## Chapter 2 Principles and Paper Review

## Chapter 3 Experimental set-up and Processes

# Chapter 4 Results and Discussion

# Chapter 5 Conclusion

# Lists of Figures and Tables

# Chapter 1. Introduction

## 1-1 Brief Review of Nanoimprint Lithography

In the past few decades , the semiconductor industry has improved dramatically and Moore's Law has been realized in a proper sequence. Until recently , scientists have realized that it's difficult to fabricate smaller structures down to sub-100 nm with optical lithography because of the diffraction effect of light. Although many semiconductor industry can demonstrate 65 nm half pitch patterns with optical immersion lithography (and the 45、32 and 30 nm half pitch patterns are in progress) , those equipments and processes are too complex and expensive. Besides , it is not clear that optical immersion lithography will be most economical when the critical minimum dimension of integrated circuits (ICs) are shrinking below 22 nm. Therefore , it is important to find out different type of lithography process to replace conventional optical lithography. In the prediction of international technology roadmap of semiconductor (ITRS) (Fig.1) , there are four candidates for sub-22nm pattern fabrication. They are extreme ultra-violet lithography (EUV)、electron beam lithography (E-Beam)、direct self-assembly innovative technology、and nanoimprint lithography (NIL). Among those lithography techniques , extreme ultra-violet lithography is still the official front runner. Electron beam lithography , which continues to be developed both for mask making and for direct writing (also known as "maskless lithography" , ML2 , Fig.2) , is limited by the low throughput. Direct self-assembly must overcome the overlay accuracy problem. Thus , NIL is a

comparatively cheap and promising process.

In 1995 , Professor Stephen Y. Chou of Princeton University invented a new fabrication way in semiconductor fabrication field. It is called nano- imprint lithography (NIL) [3]. Briefly speaking , this technique was demonstrated by pressing the patterned mold to contact with the polymer resist directly. The patterns on the mold will transfer to the polymer resist without any exposure source. Therefore , the diffraction effect of light can be ignored and the limitation is depended only on the pattern size of mold rather than the wavelength of exposure light.

Nano-imprint lithography (NIL) technology is a physical deformation process and is very different from conventional optical lithography. This technology provides a different way to fabricate nano structures with easy processes、high throughput and low cost；Currently , there are three main research of NIL techniques under investigation , which are hot-embossing nanoimprint lithography (H-NIL[3])、ultra-violet nanoimprint lithography (UV-NIL[4]) and soft lithography[5]. Those NIL technology can be applied to many different research fields , include nano-electric devices[6]、bio- chips[7]、micro-optic devices[8]、micro-fluidic channels[9]…etc..

## 1-2 Motivation and Approach of this Thesis

With the development of e-beam lithography in our laboratory , we

can easily fabricate sub-100 nm nanostructures on Si wafer、ITO glass (Indium Tin Oxide)、and quartz (or sapphire) plate. The problem is the low throughput and high cost of E-beam lithography process. Therefore , we launch an investigation on NIL technology by using e-beam writer to manufacture nanostructures on large-area NIL mold. These nanostructures are then duplicated with fast NIL process rather than using time-consuming e-beam writing processes.

In our investigation , we build up a home-made nano-imprint tool which has equipped with 150W Xe lamp、heating system、and pneumatic system. This home-made equipment can work in H-NIL、UV-NIL、and other types of NIL process (ex. Fracture induced structuring、lithographically induced self-assembly…etc.).

Currently , we can duplicate sub-200 nm nanostructures with this home-made equipment. With further improvement , we can fabricate smaller nanostructures with this facility and find applications in related fields.

(a)

|  | 2007 | 2010 | 2013 | 2016 | 2019 | 2022 |
|--|------|------|------|------|------|------|
|  | 2008 2009 | 2011 2012 | 2014 2015 | 2017 2018 | 2020 2021 | 2023 |

DRAM 1/2 Pitch    65nm

193 nm
65  193 nm immersion with water

**193nm immersion with water**
**193nm immersion double exposure / patterning**

Flash Half-pitch

45  193 nm immersion with water
45  193 nm immersion double patterning    Narrow options

193 nm immersion double patterning
EUV
32  193 nm immersion with other materials
ML2, Imprint

**193nm immersion double exposure / patterning**
**EUVL**
**193i+ with other fluids and lens materials**
**ML2, Imprint**

EUV
22  Innovative 193 nm immersion
ML2, imprint, innovative technology

16  Innovative technology
Innovative EUV, ML2, imprint, Directed Self Assembly    Narrow options

(b)

| | | | | Nanoimprint | |
|---|---|---|---|---|---|
| Technology | DUV | X-ray | Immersion | Electron Beam | Nanoimprint |
| Pattern generation | Mask | Mask | Mask | Serial Exposure | Stamp/Mold |
| Exposure area | Wafer | Wafer | Wafer | 1-10mm | Wafer |
| Min. dimension | 100 nm | 30-70 nm | ~45 nm | 3 nm | 8 nm |
| Exposure time 8 " wafer | 60-300 s | >120 s | 60-300 s | >10 h | 10-180 s |
| | | | | Master production | Mass production |

Fig.1 (a)The prediction of lithography design rules from international technology roadmap of semiconductor(ITRS)[1] and (b) the comparison of different type of lithographical methods
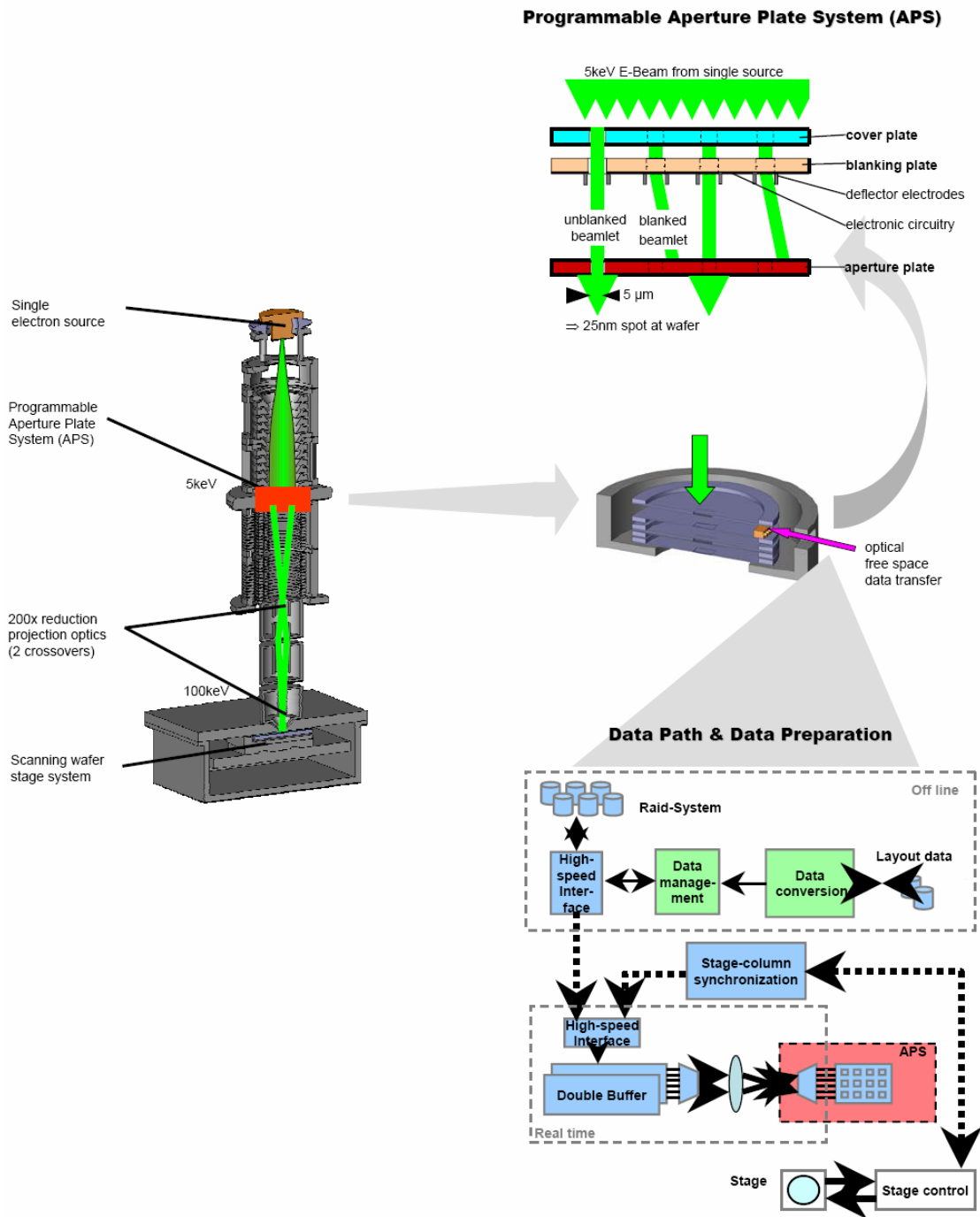
Fig.2 The overlay of the projection maskless lithography , PML2[2]

# Chapter 2. Principles and Paper Review

## 2-1 History of lithography

As the integrated circuits (ICs) patterns are becoming smaller , a variety of specific methods are needed. In the early 1960s , the ICs pattern was defined by contact lithography. But this technique is not very attractive , scientist are preferred to replace contact lithography by proximity lithography , because of the low throughput and defects which generate from the repeated contact process of contact lithography.

The proximity lithography was developed in which there is a gap between the wafer and substrate. Therefore , the optical diffraction effect and numerical aperture (NA) should be taken into consideration , as shown in Equation 1~2. In this case , the wavelength and NA are playing important roles. As the wavelength of exposure light is shorter or NA is increased , the resolution gets improved. Therefore , the requirement of shorter exposure wavelength , from G-line (436nm)、I-line (365nm)、KrF excimer (248nm)、ArF excimer (193nm)、$F_2$ excimer (157nm) to EUV exposure tool , becomes the main strategical ambition. Although , shorter wavelength exposure tools can provide smaller pattern size , however , the cost of process is becoming enormous.

Nowadays , sub-90 nm devices have been demonstrated using ArF excimer as a exposure source and collocating with immersion lithography technique by filling some specific liquid into the gap between mask and substrate to provide a better refraction index. This method can provide 65 nm half-pitch (even down to 45、32 nm) patterns and put them into mass

production. However , this equipment cost around US$30,000,000 and the extra cost of the matching process is huge. Therefore , scientists still tried hard to find out some easy and inexpensive processes to replace those conventional lithography.

$$R = k1\frac{\lambda}{NA}$$ ……………………………………………………Equation 1

R：The minimum half pitch , R , resolvable for a diffraction limited

    optical projection system

λ：Exposure wavelength

NA：Numerical aperture (which equals to $n\sin\alpha_0$)

$$DOF = k3\frac{\lambda}{n\sin^2\left[\frac{1}{2}\sin^{-1}\left(\frac{1}{n}\sin\alpha_0\right)\right]}$$ …………………………………Equation 2

DOF：Depth of focus

n：The minimum index of refraction of the imaging medium

$\alpha_0$：The maximum half angle of rays focused by the lens to the image

$k_{1,3}$：The constants which are depended on the tool, process, pattern size

    and pattern geometry.

## 2-2 Electron beam lithography system

### 2-2-1 History of electron beam lithography

In the age of 1920 , the physicist de Brogile invented the theory of matter wave , by introducing a function $\lambda = h/P = h/(2qmV)^{1/2}$ . Considering the electron , the de Brogile wavelength is $\lambda = h/P = h/(2qmV)^{1/2} = 1.22/(V)^{1/2}(nm)$. It means that the wavelength is 0.012 nm when electron is accelerated by 10kV voltage. This is much smaller than the wavelength of visible light. If we use electron wave to observe objects in stead of using visible light , theoretically , we will "see" objects more clearly and the diffraction effect will be eliminated.

By this result , Knoll and Ruska et. al manufactured the first electron microscopy in 1933. It was a transmission electron microscopy (TEM). Later , Ardenne et. al demonstrated the first scanning electron microscopy (SEM) in 1938. But the first scanning electron microscopy had bad resolution because of its poor electro-magnetic lens and electron collection system. Until 1953 , McMullan et. al built up a brand-new SEM system which was the proto type of modern SEM system , it provided better resolution and good image.

As the SEM technology became matured , Matta et. al utilized the focused electron beam as the exposure source to manufacturing the micro-electromechanical system (MEMS). And this became the first model of electron beam lithography system.

With the development of semiconductor industry , it becomes necessary to produce the smaller patterns and nano-scale structureson

devices. The electron beam lithography system plays an important role and provides a promising technology to fabricate various remarkable nanostructures.

## 2-2-2 Introduction of electron beam lithography system

Generally speaking , electron beam lithograph system is constructed from four main parts ; including electron optical column、chamber、handling system、and control unit. The major part is electron optical column , which determines the shape of electron. It controls the image resolution and exposing quality. Electron optical column is generally composed of electron gun、blanking、condense lens、stigmator、objective lens、deflector、and electron detector (Fig.3). These accessories enable the electron beam ejecting from electron gun to be well-controlled and expose to the right place.

There are three common phenomena occur during the exposure of electron beam system ; including forward scattering、back scattering、and charging effect. Each of them can influence the quality of the e-beam exposed patterns , especially when the pattern size is down to sub-50nm. The effect of forward and back scattering will broaden the pitch size and produce some proximity effect. The charging effect is the results of the electron accumulation phenomenon. These effects will blur the exposed image and produce a poor exposure quality (Fig.4).

## 2-3 Nanoimprint lithography

### 2-3-1 History of nanoimprint lithography

Nanoimprint Lithography (NIL) was first invented by professor Stephen Y. Chou of Princeton University. At the early age , they published a paper in which they created mesa and trenches with a minimum size of 25 nm and a depth of 100 nm by pressing a mold into a thin thermoplastic polymer film on substrate[3]. This method has attracted great attention from many industrial field due to the easy、low-cost and high throughput process.

After the thermal NIL technique was first introduced , lots of different imprint methods were been developed and investigated , such as ultra-violet curing nanoimprint lithography (also refereed as step and flash nanoimprint lithography , SFIL[10])、soft lithography[11]、laser-assisted nanoimprint lithography (LAN)[12]、electrostatic force-assisted nanoimprint lithography (EFAN)[13]…etc.. These methods are generally classified into three different category , include hot-embossing nanoimprint lithography (H-NIL)、ultra-violet curing nanoimprint lithography (UV-NIL) and soft lithography. The details of these techniques will be discussed individually in next paragraph.

NIL technology is a powerful method for nano- fabrication. The smallest nanostructure demonstrated by this technology was less than 10 nm. With these excellent results , NIL technology was regard as one of the next generation lithography.

## 2-3-2 Hot-embossing nanoimprint lithography

The pioneer of hot-embossing nanoimprint lithography (H-NIL) is professor Stephen Y. Chou , who first introduces thermal NIL technique. This technology quickly attracts great attentions. The imprint methods , which drive from a thermal cycle and mechanical force , are collectively referred as hot-embossing nanoimprint lithography (H-NIL) , as shown in Fig.5.

A thermal cycle , which exercise during the imprint progress , is applied as the driving force to mobilize the polymer resist. Before the thermal cycle , the thermoplastic polymer resist is in a solid state , also named as Glassy State , at room temperature. When heating it up , the polymer reaches the glass transition temperature (Tg) and the polymer chain becomes squirming and fluidic. By supplying mechanical fore (or pressure) to contact the mold and substrate , the fluidic polymer coating on substrate will become mobile and fill into the nanostructures which were fabricated on mold. With the help of cooling and separating of mold with substrate , the patterns on the mold are transferred onto polymer resist. These transferred patterns are complementary to the patterns on mold. In virtue of some post- semiconductor progress such as reactive ion etching or lift-off process , the patterns on polymer resist can be transferred to the substrate permanently.

The most important issues of H-NIL are temperature control and separating method. The temperature governs the kinetics of polymer

chain. The most appropriate temperature for H-NIL is about 20~30℃ above Tg (Glass transition temperature)[14]. With the lower temperature , it is difficult to mobilize the polymer and it's necessary to provide much more pressure to press the mold into the polymer resist. On the other hand , the higher temperature tends to decompose the polymer , which will greatly influence the properties of the polymer , and produce more defects.

There is another technique called laser-assisted nanoimprint lithography (LAN , as shown in Fig.6) , which was also presented by professor Stephen Y. Chou. This technique uses a pulsed laser to generate a short-lived high temperature , which can rapidly melt the surface of silicon wafer , on local area , in few nanoseconds. In the mean time , by applying a giant force to contact the mold with silicon substrate , the nanostructures on mold can be pressed into silicon. After cooling and releasing the mold , the nanostructures are transferred to the silicon substrate directly without any polymer resist. Despite the expensive cost of equipment , this method provides a high efficiency process which the nanostructures are transferred without further etching process.

## 2-3-3 Ultra-violet curing nanoimprint lithography

Ultra-violet curing nanoimprint lithography (UV-NIL) was first introduced by professor M. Bender and M. Otto of RWTH-Aachen university[16]. The materials of UV-NIL is very different from H-NIL. The polymer resist for UV-NIL was UV photo-sensitive polymer. Generally speaking , the polymer for UV-NIL is the chemical cross-linking and

curing polymer when exposing with the UV light. Therefore , this method can be exercised at room temperature.

The polymer for UV-NIL are generally fluidic、photo-polymerization and low molecular weight polymer at room temperature. When exposing UV light after squeezing the polymer into patterned mold , the polymer will cure (or cross-link) along the morphology of the nanostructure on mold. Without the high temperature thermal cycle or high mechanical driving force , the polymer will just cross-link without any intrinsic transformation of polymer (i.e. glass transition or crystallize…etc.) , and it produces results with less defects in UV-NIL.

Theoretically , UV-NIL should be a more powerful technology for nano-fabrication than H-NIL. But there are still lots of difficulties when exercise the UV-NIL , such as mold fabrication、anti-sticking layer coating、UV-NIL resist selection…etc.. Professor C. G. Wilson and S. V. Sreenivasan demonstrate a method to further improve polymer resist spraying manner , which was called step and flash imprint lithography , as shown in Fig.7. Instead of spinning coat of polymer resist , this method dispenses polymer resist drop into the gap of the mold and substrate when the mold and substrate are in proximity. With the help of step and flash , the imprint patterns could be aligned with satisfactory. Despite the higher cost , UV-NIL is better in manufacturing large area patterns than H-NIL. The problems of shrinkage、adhesion and capillary bridge are not apparent in UV-NIL.

On the other hand , Chou et. al has invented an amazing technology ,

called electrostatic force-assisted nanoimprint (EFAN)[13] , as shown in Fig.8 , which replace the mechanical force with the electrostatic force. With the applying of electrostatic force between mold and substrate , the force can be uniformly applied around the whole area because of the distribution property of the electrons.

### 2-3-4 Soft lithography

Soft lithography (also called microcontact print , μ-CP) was introduced by professor G. M. Whitesides[11]. This method was a combination of imprint technology and self-assembly monolayer (SAM) technology；The process begins with a patterned master that is fabricated by conventional lithography and semiconductor process. The master is then treated with an anti-adhesion SAM before casting and curing. The elastomer material which is usually polydimethylsiloxane (PDMS). Finally , the elastomer mold was carefully peeled from the master.

Different from H-NIL and UV-NIL , the elastomer mold was used to transfer molecules of the "ink" (usually thio…etc.) to the substrate by gently contact. After imprinting , a different SAM will form by washing the substrate with the second type of molecules. This SAM patterns will keep off the chemical corrosion when the substrate was proceeded with wet or dry etching.

Soft lithography is a low pressure and low temperature process. With the formation of SAM , it provides a well-organized and high stability pattern. Additionally , with selecting of right molecules , the SAM

patterns might provide an opportunity to be a bio-sensitive or chemical-sensitive detector.

## 2-3-5 Fracturing induced structuring

Low cost and high-throughput patterning of nanostructures is essential to the fabrication and commercialization of a variety of nanodevices. NIL technique is one of the candidates which can produce nanostructure in an easy and inexpensive way. However , the key part of NIL technique is the mold fabrication. The mold with nanostructures on it are generally expensive and complicate to be fabricated. In 2007 , Chou et. al introduce a easier method to fabricate nanogratings[17]. In replacement of the mold with a blank substrate , this improved H-NIL was proceeded by two blank substrates. With carefully peeling off the two substrates , the polymer inside the gap of two substrates will stick on both of the two substrates and fracture into nanogratings.

The mechanism of FIS appear to be the same with crack propagation of polymer. From the investigation of Chou group , they claimed that the period of the FIS grating depends solely on the film thickness , scaled as $period = (4.0 \pm 0.6) * filmthickness$ . And this relation and the morphology of the grating is more clear when thicker resist film was used. On the other hand , polycrystalline materials can not fracture into grating and the highly cross-linked polymer are also not suitable for this structuring method because of the intrinsic properties of those polymers.

## 2-3-6 Related technologies

In recent years , NIL has attracted many attentions and there are many scientist investigate in this technology. Here , we discuss some unique techniques which might promote the progress of NIL in the future.

First , as we mentioned in previous paragraph , the main limitation of the pattern size is dependent on mold fabrication method. Therefore , prof. James R. Heath invented a new method[18] [19]. Instead of conventional electron beam lithography patterned mold , they employ molecular beam epitaxy (MBE) to produce a $GaAs/Al_{0.8}Ga_{0.2}As$ superlattice structure. By the selective etching in HF acid , the ultrathin $Al_{0.8}Ga_{0.2}As$ layers will be etched faster than the GaAs layers. After the selective etching , the GaAs layer structure becomes a ultrathin nanowire structure. The method can provide a convincing ultrathin nanowire structure (even down to 5nm) mold because of the MBE ultrathin film deposition capability , as shown in Fig.11.

Second , NSL (Nano-sphere lithography) technology is another common technique for the fabrication of photonic crystal or anti-reflection layer of solar cell. As polymer (such as polystyrene 、 PMMA…etc.) nano-sphere (~100-800 nm) solution dispensing on the substrate , those polymer nano-sphere will self-align above the substrate. After drying and etching the substrate , good quality nanostructures appear because those polymer nano-sphere serve as a good quality polymer mask , as shown in Fig.12.

The third , Fan and Buriak et. al[20] use the self-construction property

of the different polymer chain in copolymer (ex. PS-b-P2VP) to produce a self-aligned pattern. By the confinement of a nanostructure , the polymer chain in copolymer will self-aligned along the nanostructure. In their investigation , they can fabrication sub-10 nm patterns on silicon , as shown in Fig.13.

The techniques shown above are the most recent technologies , which are assisted with nanoimprint lithography to fabricate sub-100 nm nanostructures. All of them are easy and inexpensive than the conventional lithography. If we can handle these techniques and combine them with nanoimprint lithography , we will have a powerfully techniques on nano-fabrication.
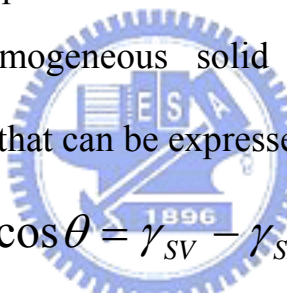
2-4 Anti-sticking layer

2-4-1  Wettability


Contact angles of liquids on a polymer surface are widely used to predict wetting and adhesion properties of these solid surfaces by calculating their solid-vapor surface energy. Using goniometry is a simple and fast way to measure the hydrophoilicity or hydrophobicity of surface. The reason for contact angle phenomena is very complicated but it is a powerful tool for making distinctions among coating properties , especially of polymer surfaces.

When a liquid drop is in contact with an ideally smooth , undeformable , and homogeneous solid (Fig.14) , it exhibits an equilibrium contact angle that can be expressed by Young's equation：

$$\gamma_{LV} \cos\theta = \gamma_{SV} - \gamma_{SL} - \pi_e$$

where $\gamma_{LV}$ is surface tension of the solid in equilibrium with its own vapor ,

$\gamma_{SL}$  is interfacial tension of the solid in equilibrium with the saturated

liquid vapor and  $\theta$  the contact angle , and  $\pi_e = (\gamma_S - \gamma_{SV})$ is equilibrium

pressure.


2-4-2 Fabrication methods of anti-sticking layers


The separating form is also vital in NIL tecnique. One of the most common observed defect generation sources is the stiction properties between ultrathin polymer layer and mold during and after the embossing process. The common way to overcome this problem is applying an

anti-sticking layer onto the mold. There are four common strategies to apply anti-sticking layer，include spin coating、liquid self assembly monolayer (SAM)、vapor SAM、plasma polymerization，the comparison of those methods are shown in Table 1.
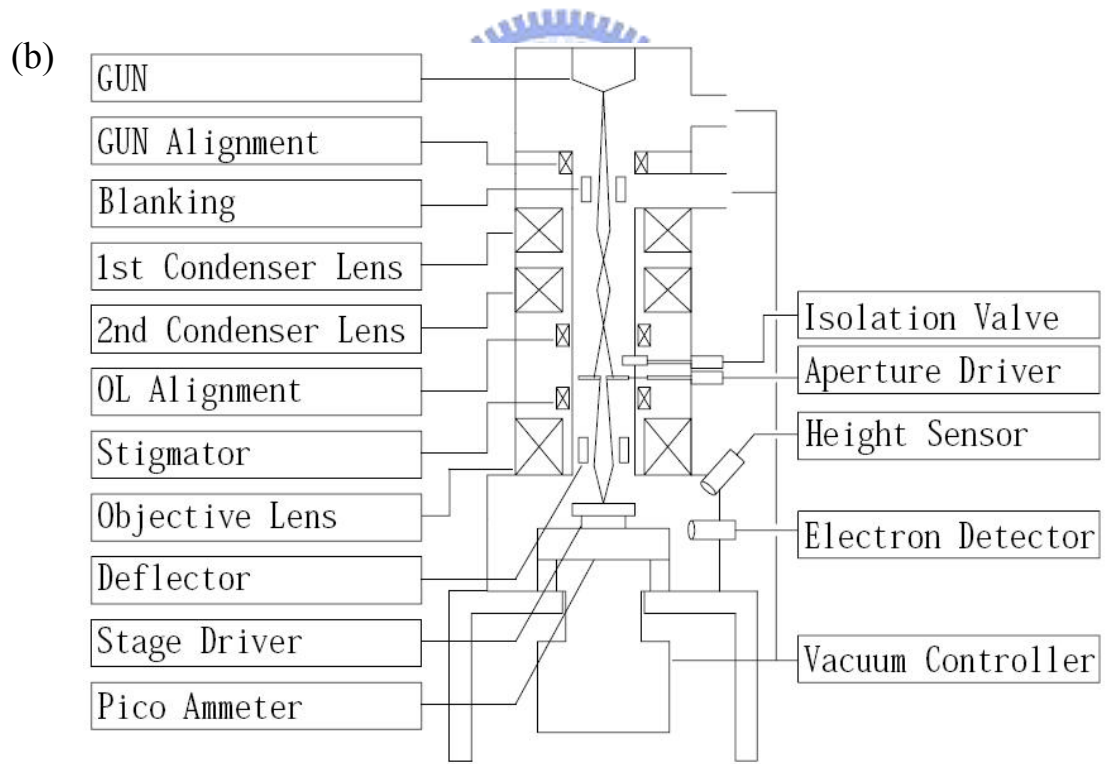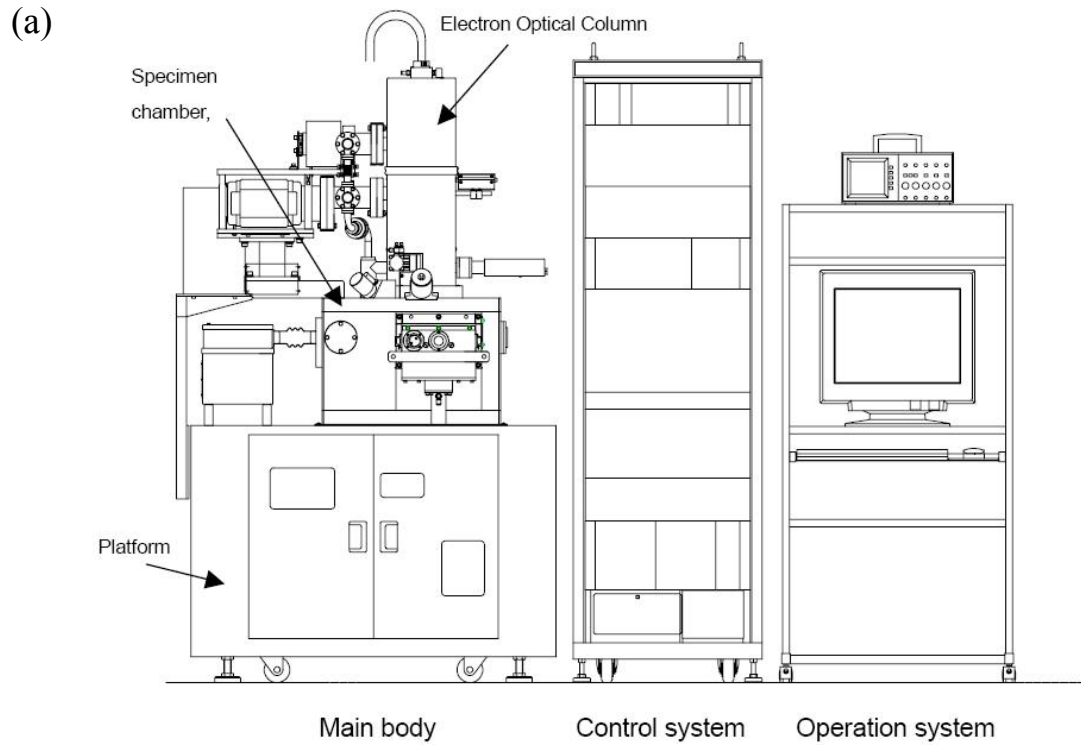
Fig.3 (a) The overlay of electron beam system (b) The overlay of electron
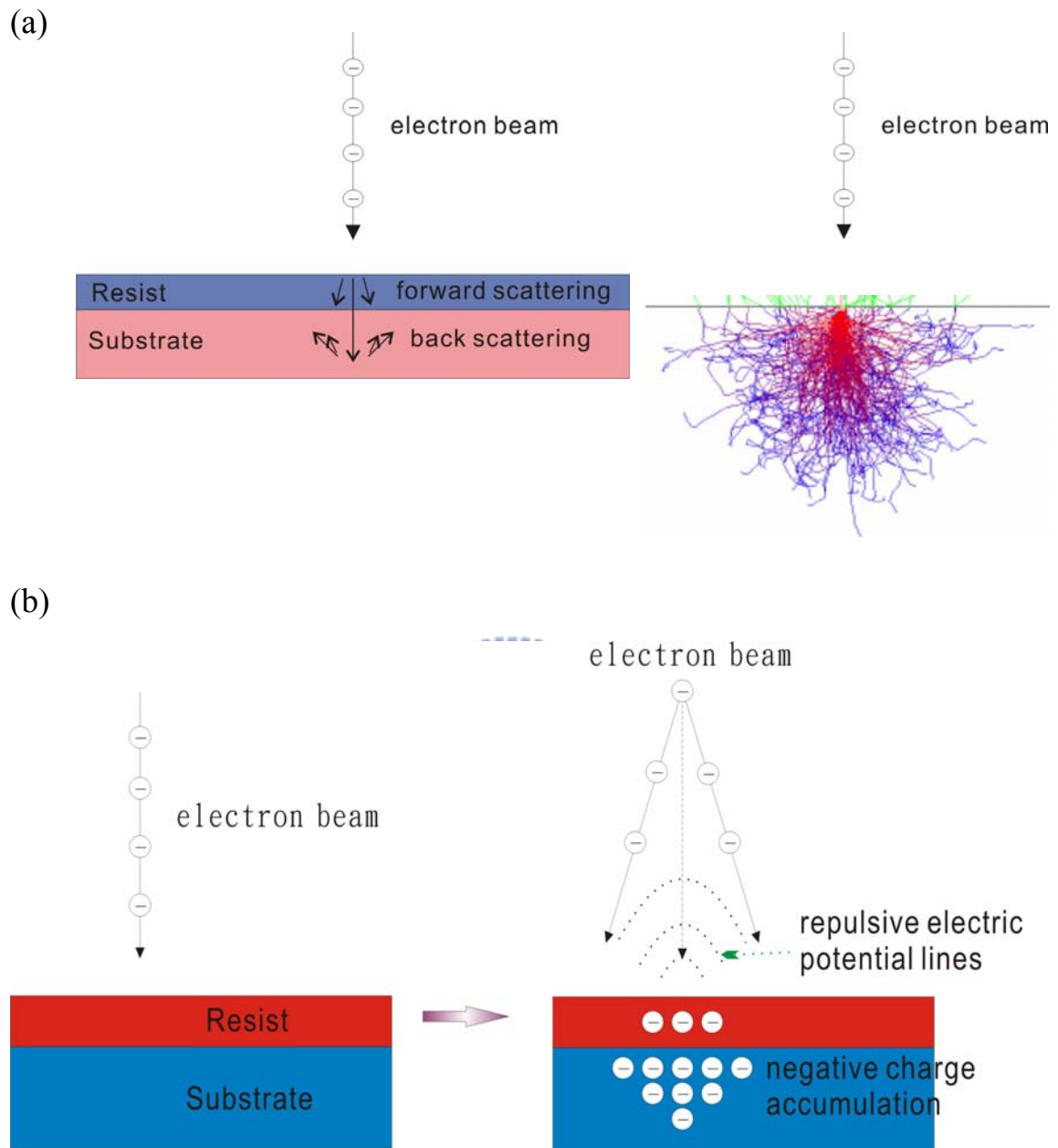optical column of electron beam system

(a)



(b)



Fig.4 (a) The illustration and simulation result of forward and back
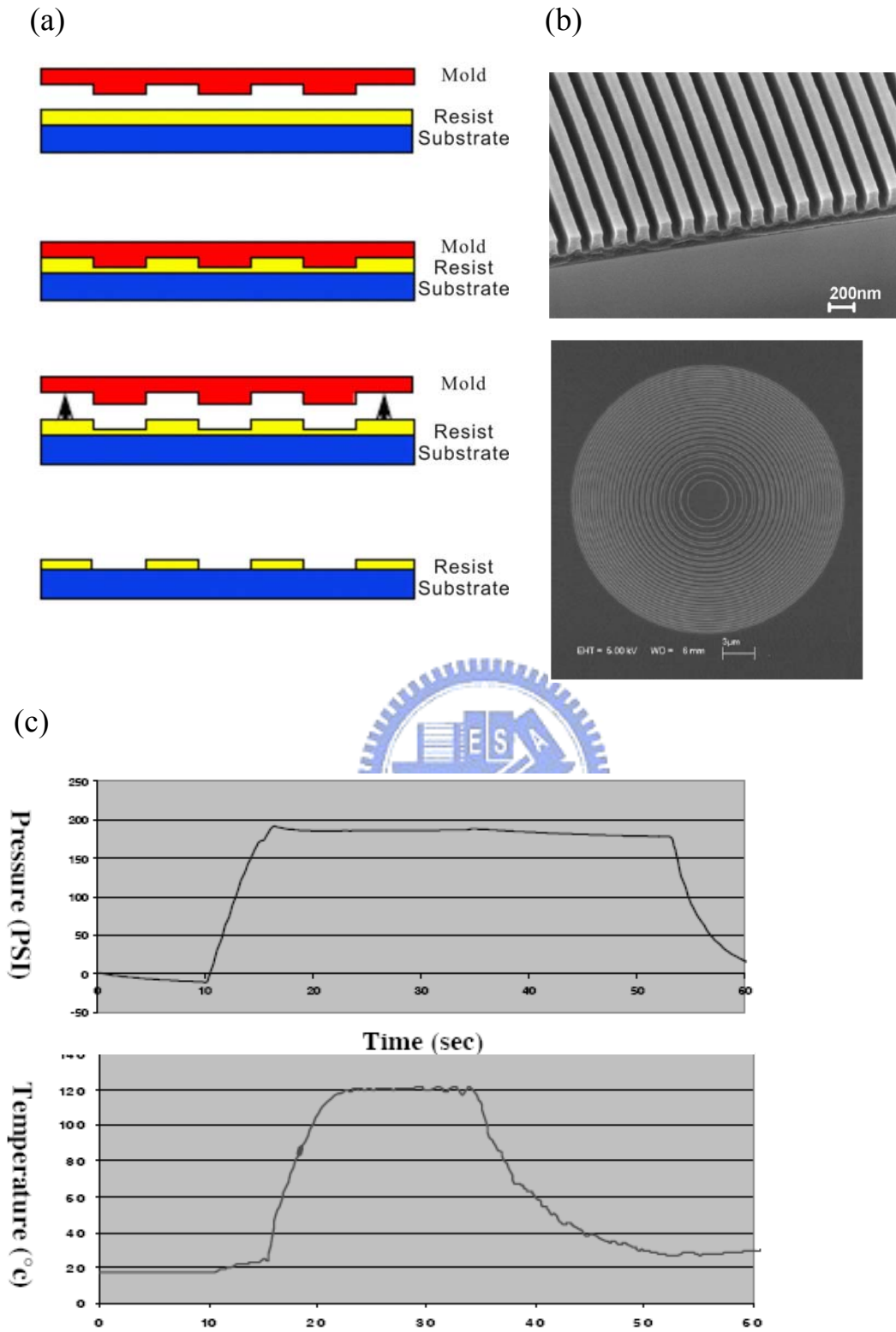scattering effect (b) the charge effect during the electron beam
process

(a)

(b)

(c)

Fig. 5 The (a) process flow (b) results (c) process parameter of
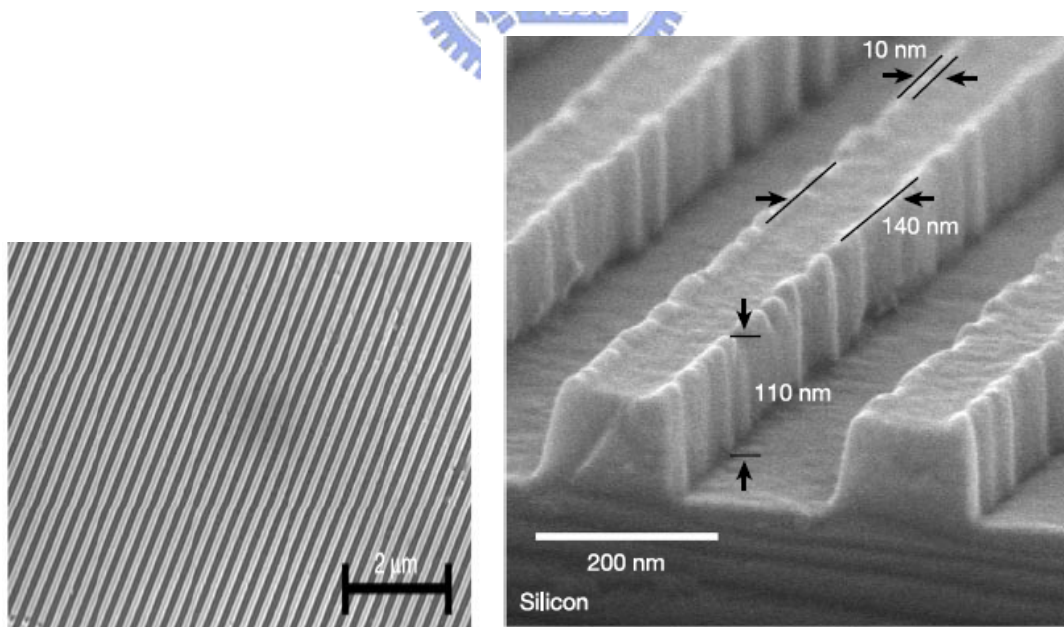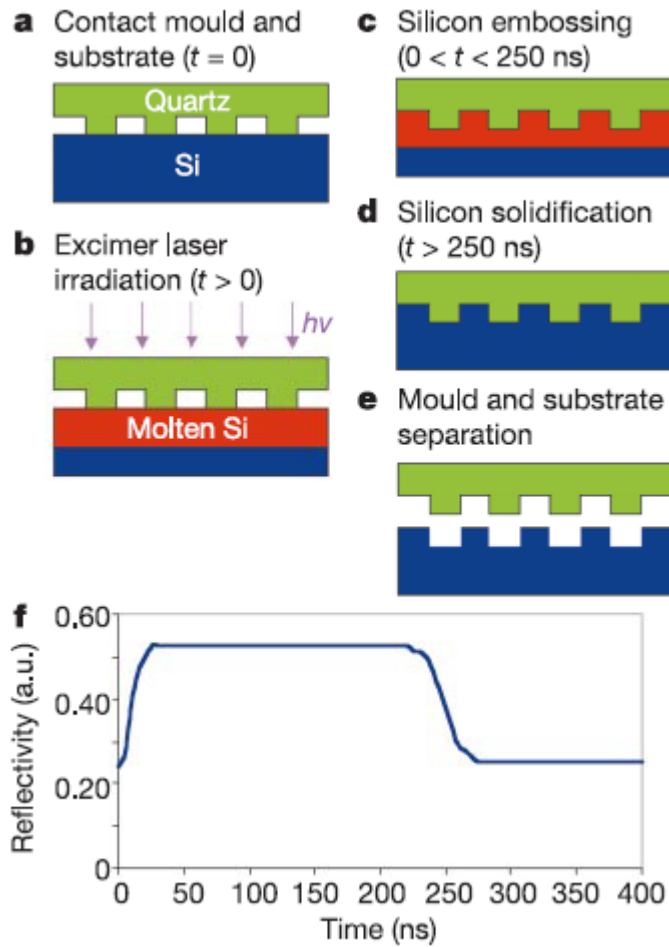
hot-embossing nanoimprint lithography (H-NIL)[15]

22

**a** Contact mould and substrate ($t = 0$)

Quartz

Si

**b** Excimer laser irradiation ($t > 0$)

$hv$

Molten Si

**c** Silicon embossing ($0 < t < 250$ ns)

**d** Silicon solidification ($t > 250$ ns)

**e** Mould and substrate separation

**f**

Reflectivity (a.u.)

Time (ns)

2 μm

10 nm

140 nm

110 nm

200 nm

Silicon

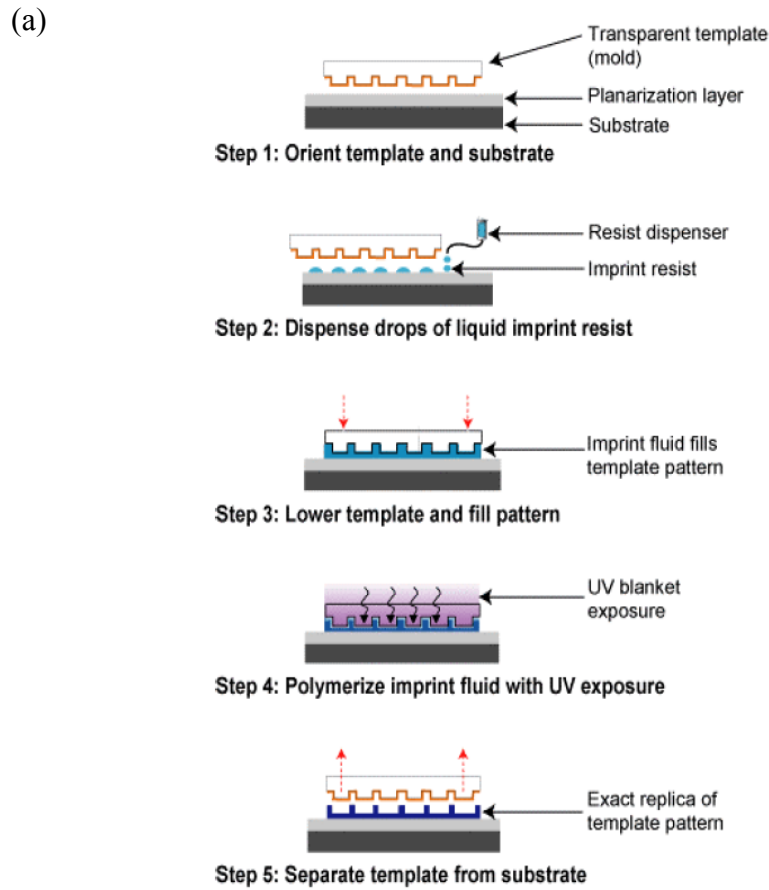Fig. 6 The process flow of laser-assisted nanoimprint lithography (LAN) and the LAN results[12]

23

(a)



(b)
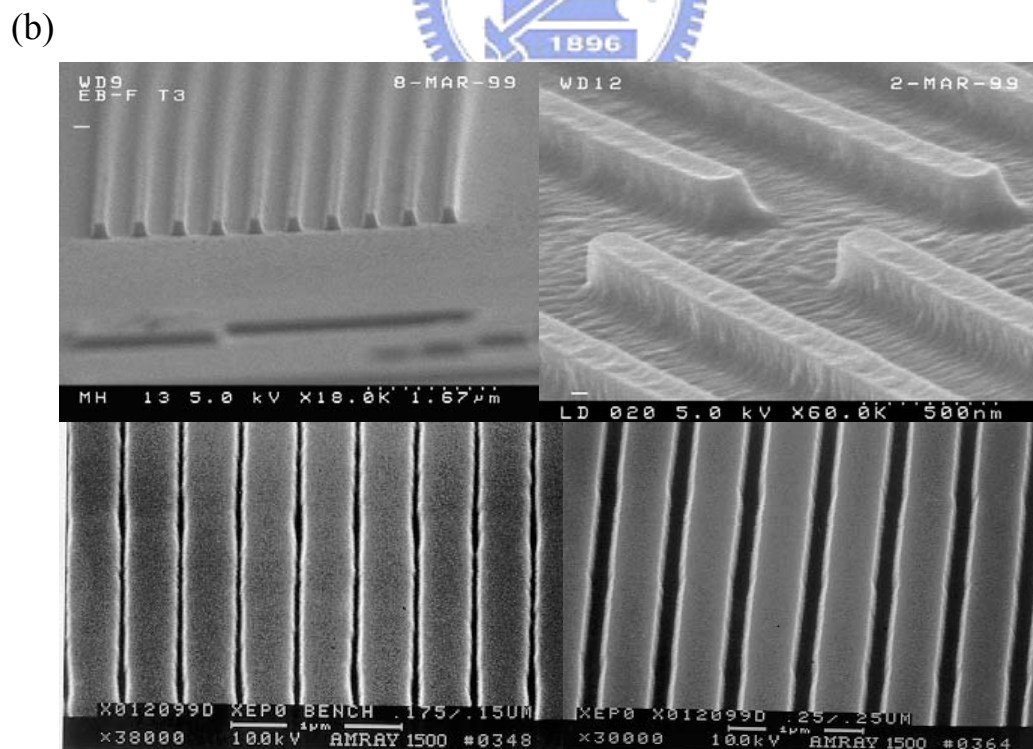


Fig. 7 The (a) process flow and (b) results of step and flash imprint
lithography[10]

24

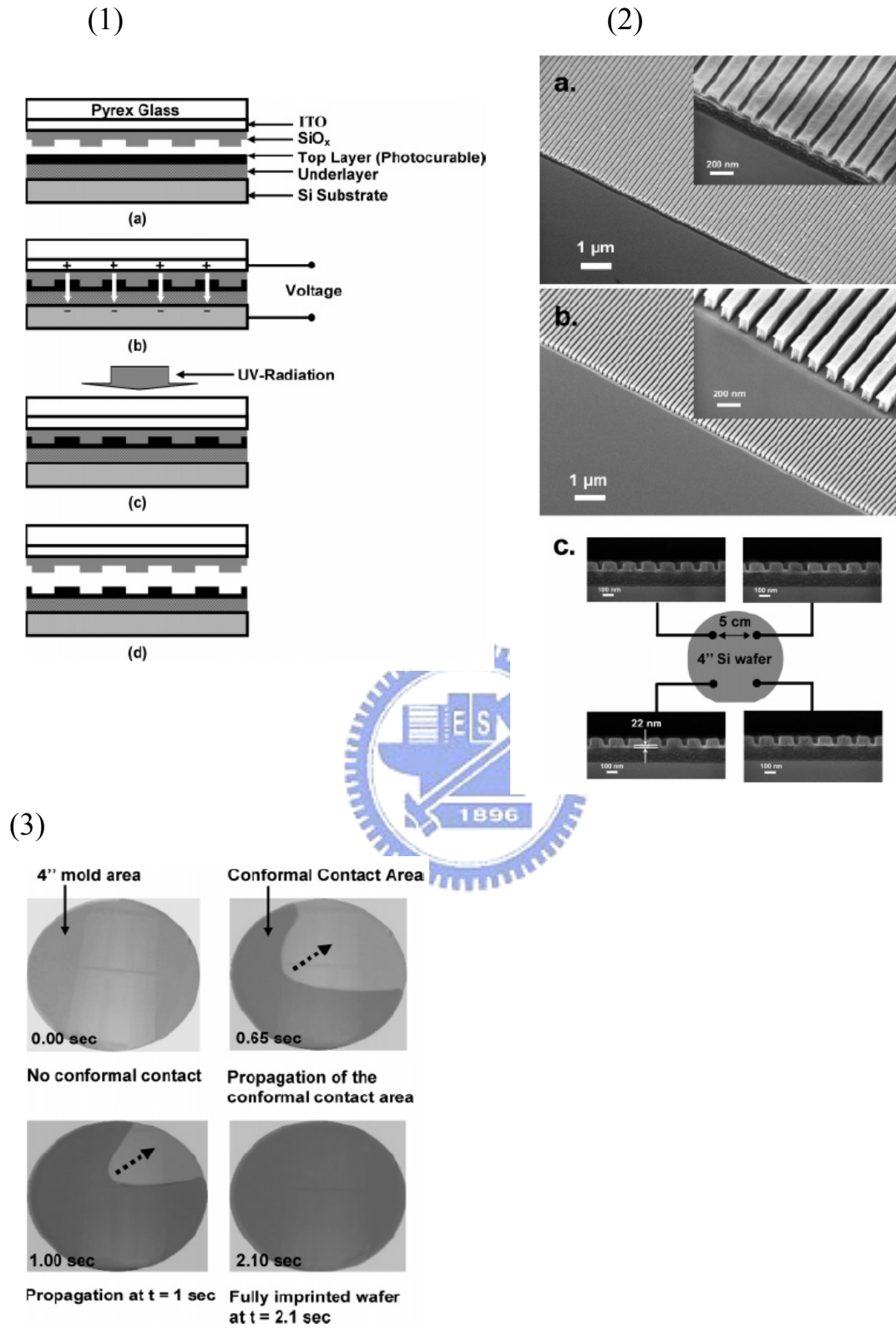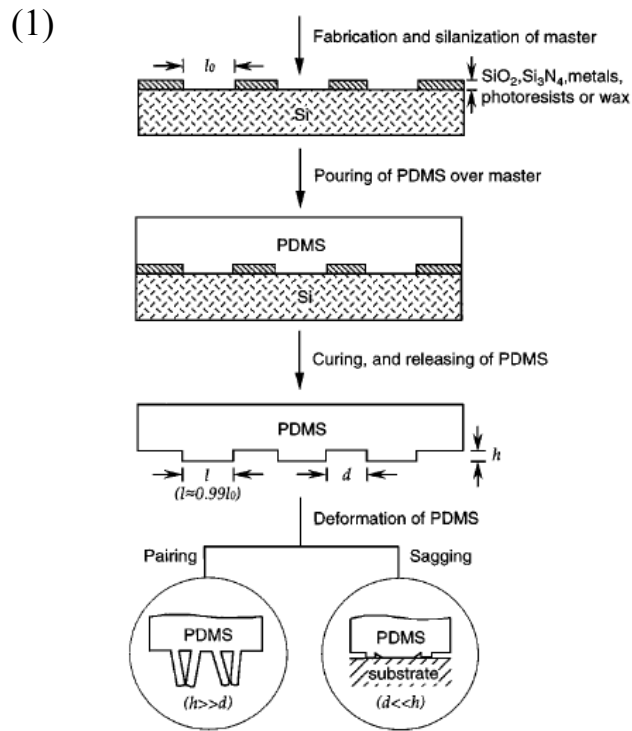(1)                                                    (2)



(3)



Fig. 8 (1)The process flow of Electrostatic force-assisted nanoimprint

(EFAN) (2) the results of EFAN (3) the photograph of the

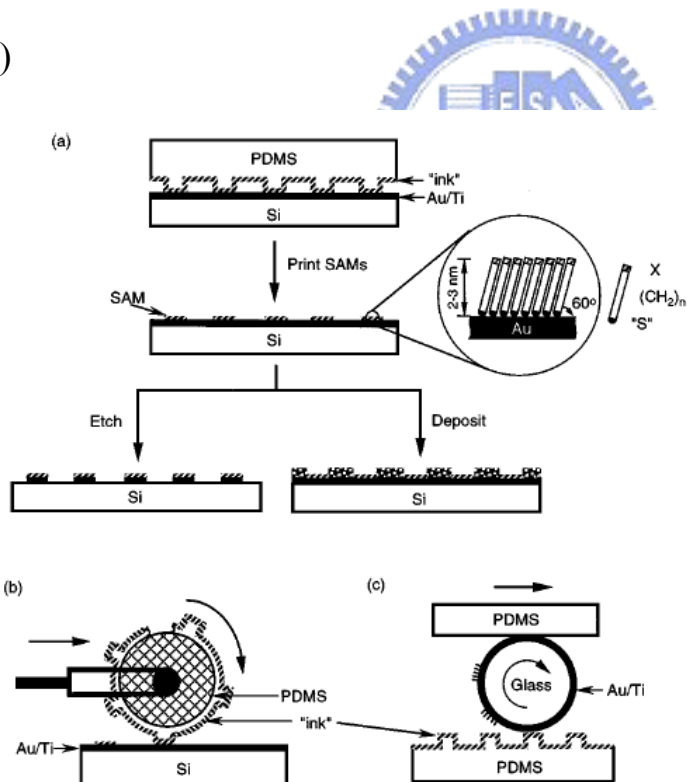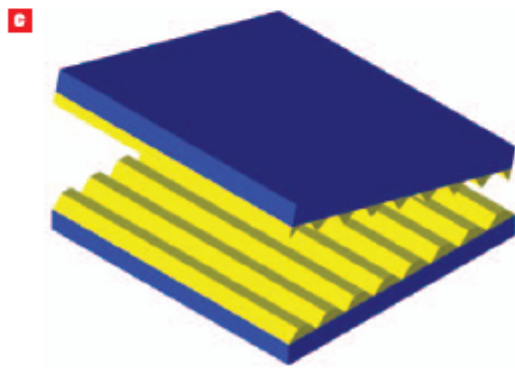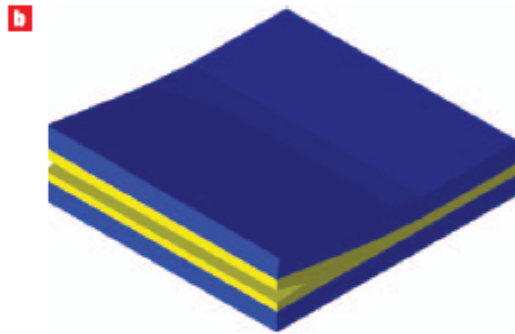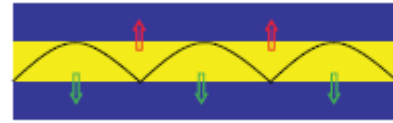uniformity of 4 inch full wafer[13]

Fig. 9 (1) The process flow of mold fabrication of soft lithography (2)

three different types of transfer process of soft lithography[11]

(1)



(2)



(3)


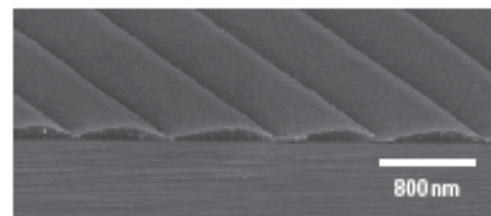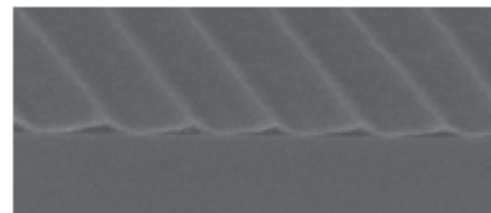
Fig. 10 (1) The process flow of FIS (2) the illustration of the separation model (3) the results of FIS[17]
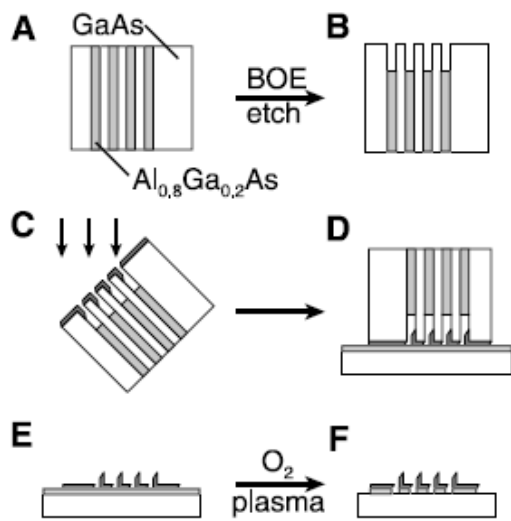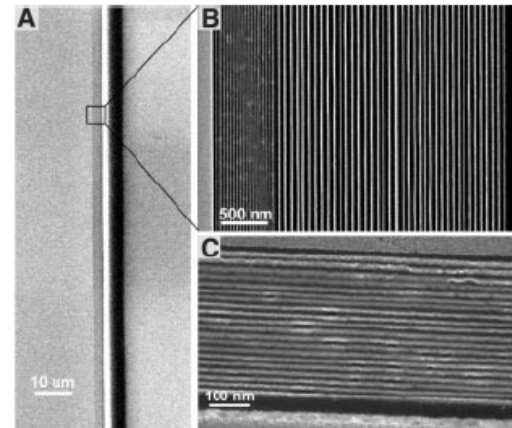
Fig. 11 (1) The process flow of assembly of metal grating by MBE superlattice mold nanoimprint lithography (2) the results of this process[19]
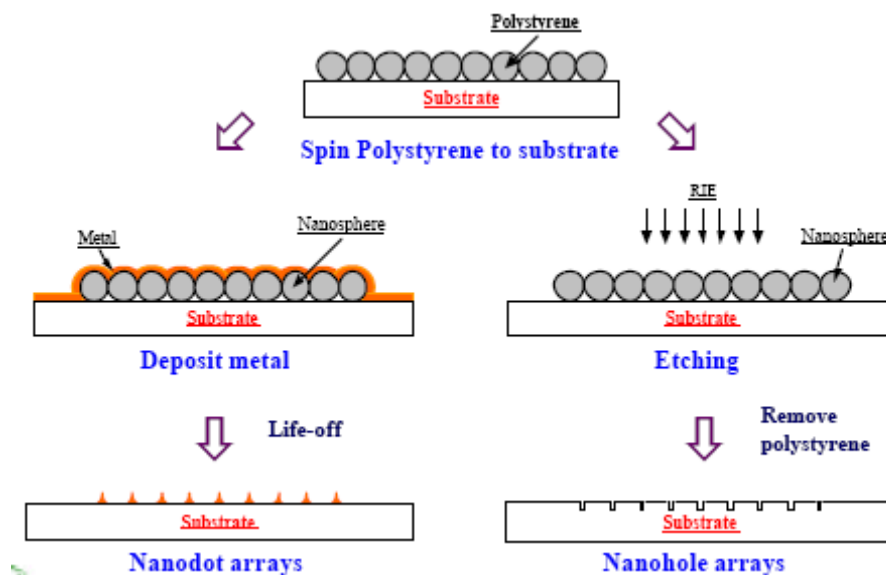


Fig. 12 The process flow of nano-sphere lithography

(1)
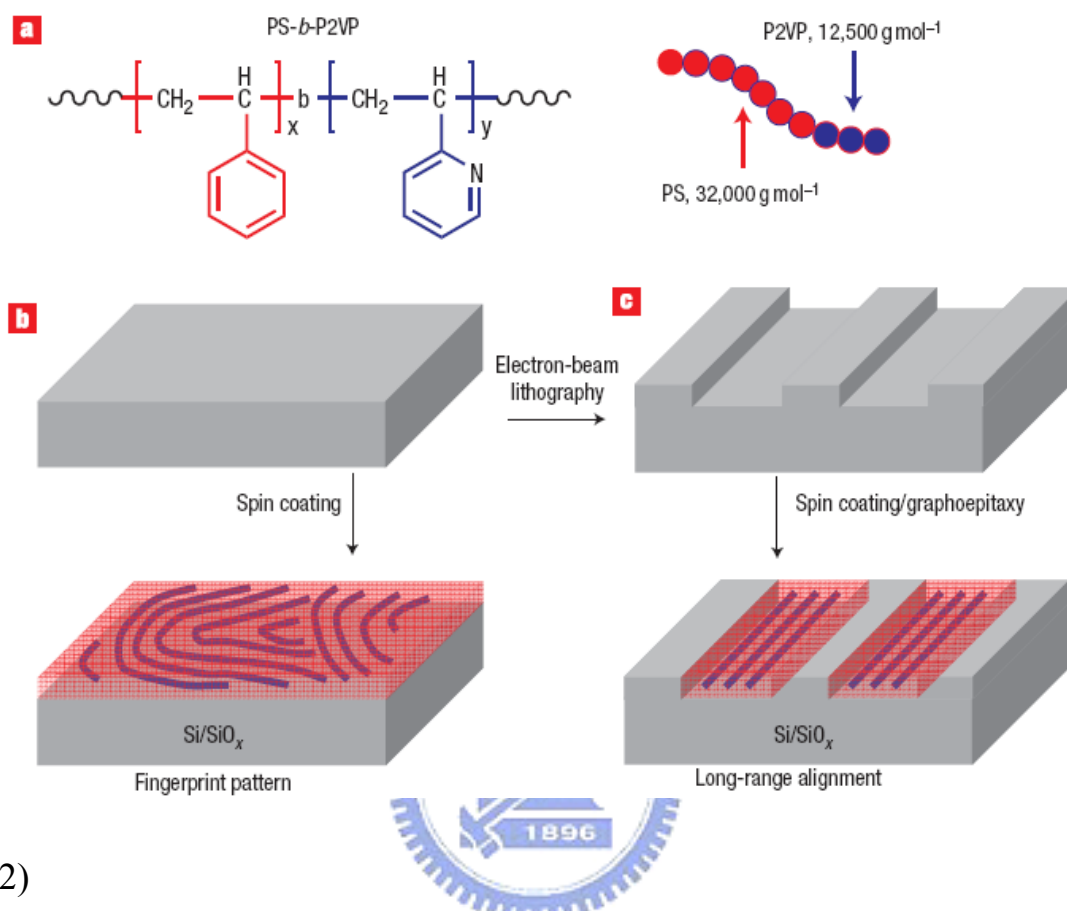


(2)
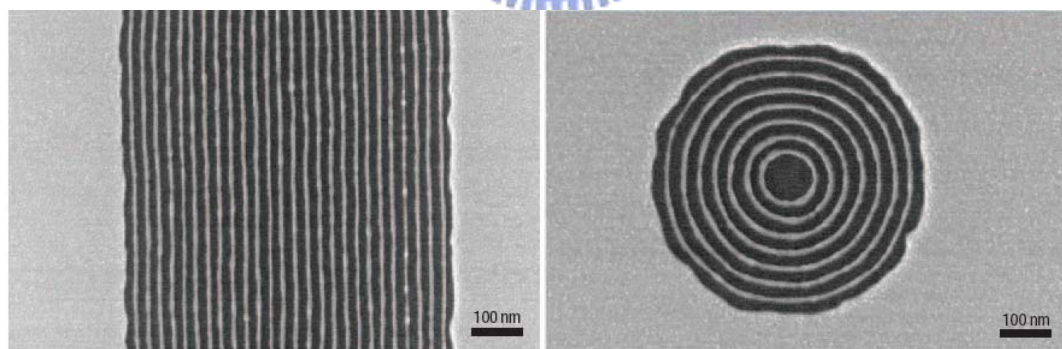


Fig. 13 (1) The process flow of assembly of aligned patterns on silicon (2) the results of assembly of aligned patterns with a confinement of nanostructure[20]

(1)
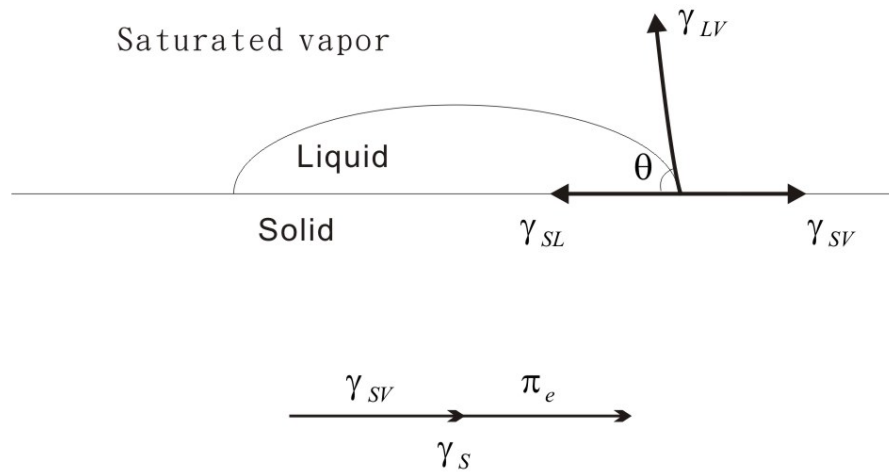


(2)
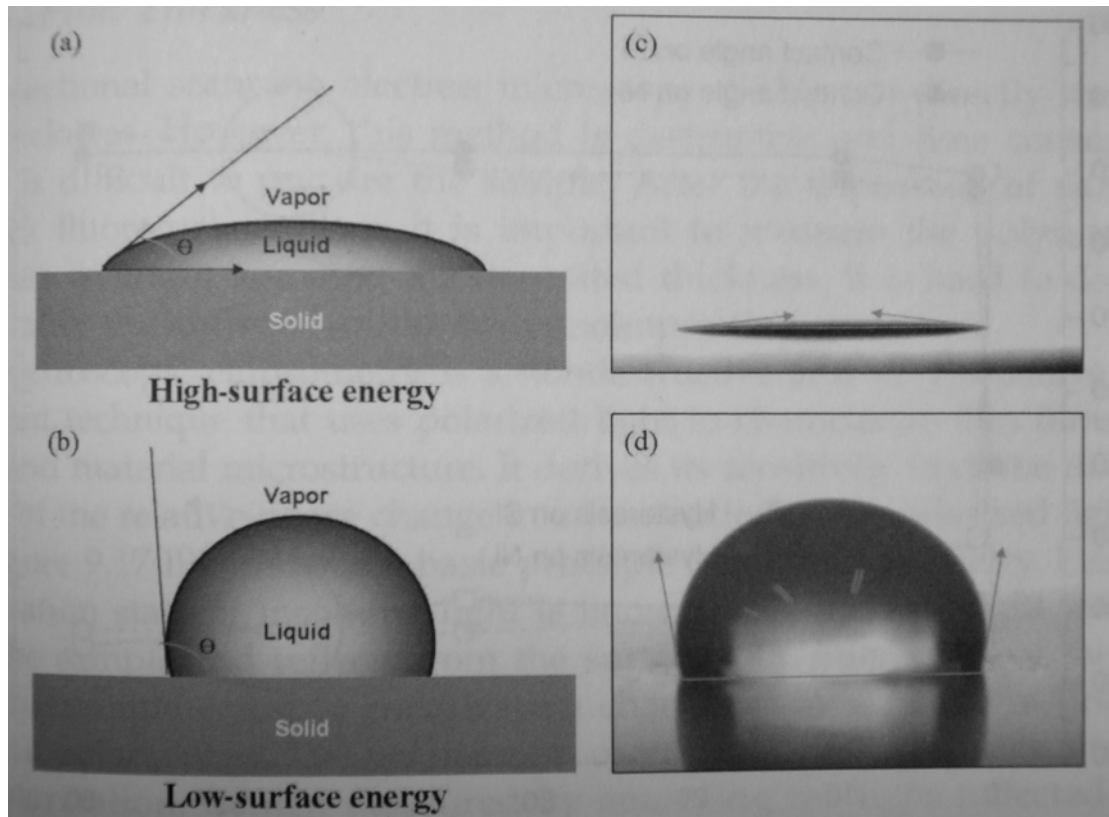


Fig. 14 (1) A sessile drop of liquid on a solid showing a three-phase force
lin (2) Schematic diagram of (a) high-surface energy and (b)
low-surface energy. Photograph of (c) low contact angle ($\sim 5^{\circ}$) and
(d) high contact angle ($\sim 108^{\circ}$)

# Chapter 3. Experimental set-up and Processes

## 3-1 Introduction of home-made nanoimprint system

With the development of e-beam lithography in our laboratory , we can manufacture many different type of nano-scale structures. However , e-beam writing is a time–consuming process. For example , it might cost a whole day to fabricate nano-scale patterns in an area of only a few $cm^2$. Therefore , we developed a home-made nanoimprintor and combine it with the e-beam and NIL technology to fabricate large-area nanostructures in a fast manner.

At the beginning , we designed a vacuum chamber with the size of $30*30*30$ $cm^3$ which was equipped with the sliding track system、 bellow、and air pressure system. The air pressure system was constructed with two separated vacuum parts , as shown in <span style="color:red">Fig.15</span>. After pumping down both parts of the chamber , the NIL pressing force is generated by venting the upper vacuum part. During a couple of tests , we figured that this design is not suitable for NIL experiments. Because the imprint force is always in 1 atm (~0.1MPa , max.). Besides , the impact between mold and substrate is huge because it is difficult to control the sliding speed of the track during the venting of the upper vacuum part. Thus , we always got damaged or broken molds and substrates after imprinting. Therefore , we decided to change our design and make this facility more controllable.

We replaced the air pressure system with a pneumatic system. With the pneumatic system , the imprinting force is highly improved up to 0.8 MPa (max.). And the bumper inside of the pneumatic system can buffer

the impact during the imprint process , as shown in Fig.16. Besides , we added three additional springs around the stage and a ball bearing stick in the middle of the stage to buffer and reduce the impact.

We put three cartridge heaters inside the stage to control the temperature during the imprinting process. The heating rate is about 40℃/min (up to 300℃). And this heating system was controlled by PID (proportional-integral and derivative) controller. Additional , the cooling rate is about 60℃/min using a water bath.

The 150W Xenon lamp、condensed lens and manual shutter are added to the system to provide the UV exposure. Theoretically , we can get about 10% light intensity (300-400 nm wavelength UV light) from the total output of the Xenon lamp. The available exposing dose for crosslinking or curing of the UV resist is 150W * 10% * $(0.9)^3$ * 0.7/ $\pi$ *$1.5^2$ = 1.0834 W/cm$^2$ (where 0.9 represents the transmission rate of quartz windows and condensed lens；1.5 represents the exposing area；0.7 represents a hypothetical light decreasing through the long distance). By controlling the exposure time , this light source can be used for most UV-NIL resists , such as PAK-01 and SU-8…etc..

Finally , by putting all the parts together , we built up a home-made nanoimprintor , the layout of this equipment is shown in Fig.17. As our expectation , we can duplicate nanostructures with this home-made nanoimprintor in H-NIL、UV-NIL、thermal and UV combined technique、(or even soft lithography)…etc.. With this equpiment , we

investigated in many different NIL method, and presenting these processes and results in the following paragraph.

## 3-2 Electron beam lithography

### 3-2-1 Introduction of electron beam lithography system

The system of electron beam lithography that we exercise is ELS-7500EX. The system was equipped with ZrO/W thermal field emission (or Schottky) Gun and high acceleration voltage up to 50 kV. The electron beam shape is Gaussian Type. The resist for e-beam process is ZEP-520A (copolymer of α-chloromethacrylate and α-methylstyrene, Fig.18). It is a high resolution、high sensitivity and good etch resistance positive e-beam resist.

We can fabricate many different patterns, such as grating、hole array、or starlike patterns…etc., with structure size down to sub-50 nm, as shown in Fig.19~21. However, the main purpose of the e-beam lithography system is to manufacture nano-scale patterned mold which will be utilized in large area H-NIL and UV-NIL transfer process. Therefore, for the convenience of fabrication and observation, we almost used nano-scale grating patterns in our research.

The substrate、exposure parameters and post-process are slightly different between thermal and UV type mold fabrication process. Therefore, both NIL mold fabrication processes will be shown in detail in the following.

## 3-2-2 H-NIL mold fabrication process

The most common substrate used for H-NIL mold fabrication in our laboratory is the Si wafer because Si wafer is easy to handle in the fabrication process. Process flow and illustration are shown below：

(1) Clean up the substrate with acetone(ACE)、isopropanol(IPA)、D.I. water by ultrasonic agitation

(2) Spin coating electron beam resist , ZEP-520A

(3) Exposing by electron beam writer

(4) Develop by ZED-N50

(5)Alternative with Lift-Off (for rising patterns , Fig. 22) , or RIE process (for depressing patterns , Fig. 23~24)
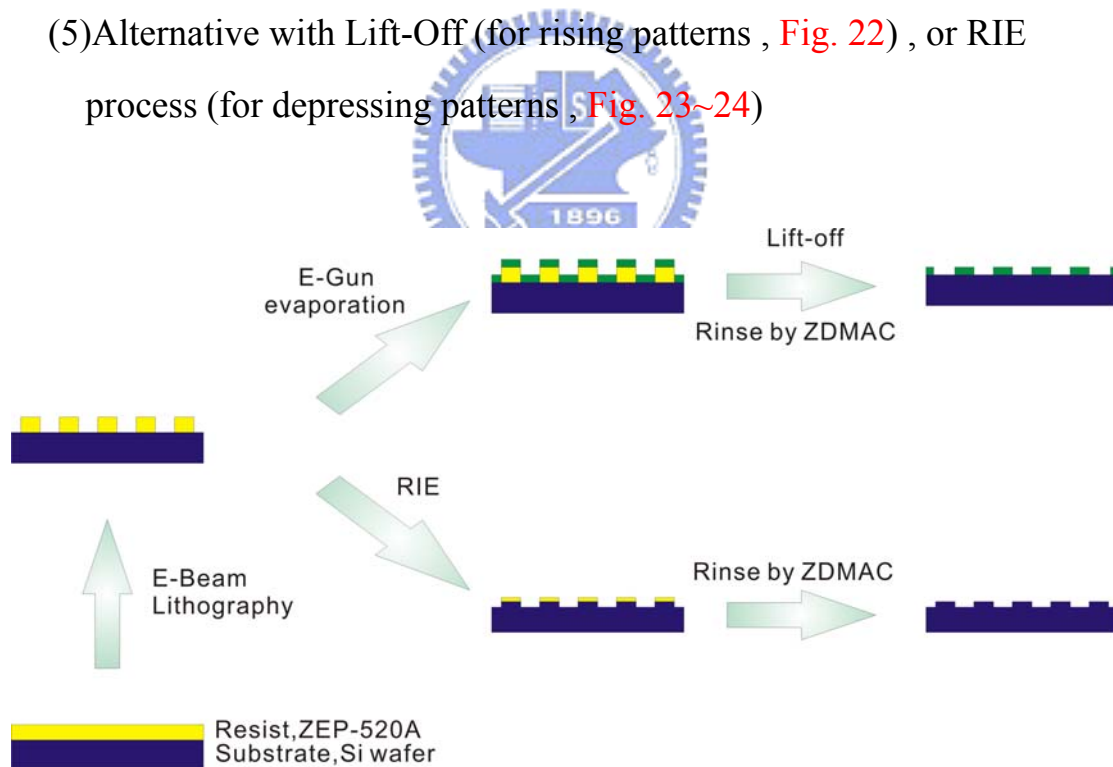


## 3-2-3 UV-NIL mold fabrication process

The UV-NIL mold fabrication process is different from H-NIL

34

because the mold for UV-NIL should be transparent. Although we can expose e-beam pattern on quartz plate sputtered with Al ultrathin film , the post trilayer etching process is not reliable with the available HDP-RIE system. Therefore , we use the ITO glass plate as the substrate and combining with the Lift-off technique to produce the UV-NIL mold (Fig. 25). Process flow and illustration are shown below：

(1) Clean up the substrate with ACE、IPA、D.I. water by ultrasonic

(2) Sputtering metal thin film (conducting layer) on quartz plate

(3) Spin coating electron beam resist , ZEP-520A

(4) Exposing by electron beam writer

(5) Develop by ZED-N50

(6) Lift-Off (rinse by ZDMAC)

Lift-off
Rinse by ZDMAC

E-Beam
Lithography

Resist,ZEP-520A
Substrate,ITO glass

E-Gun
evaporation
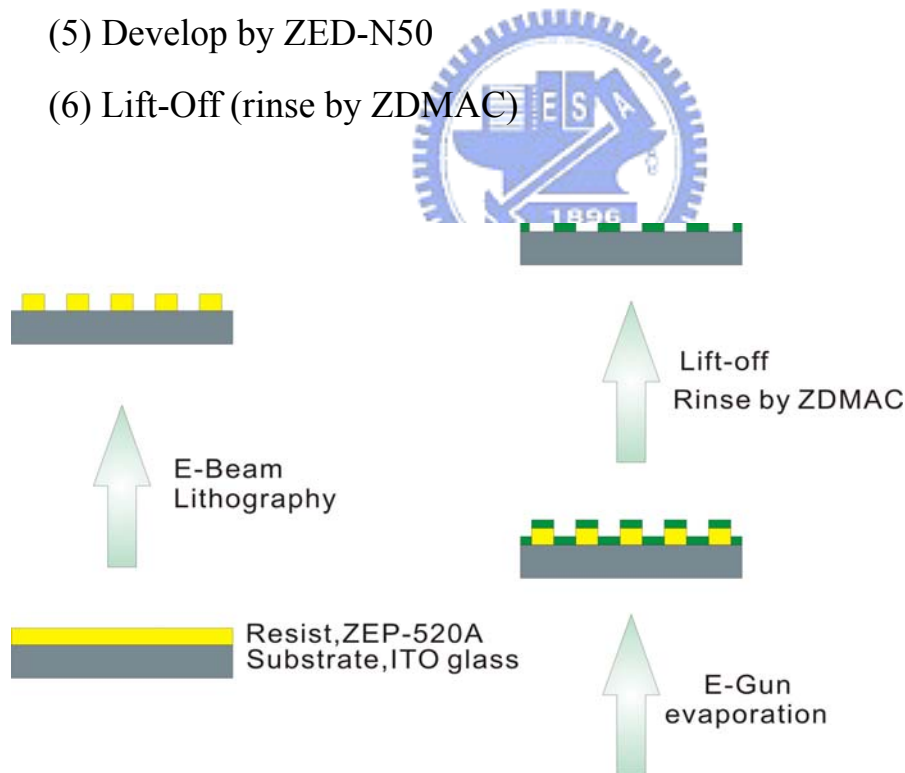
## 3-3 Nanoimprint lithography

### 3-3-1 H-NIL fabrication process

The thermoplastic polymer are chosen of poly-methyl methacrylate (PMMA , Fig. 26) with molecular weight around 495,000(495k). This resist provide high resolution for H-NIL. Process flow is shown below：

(1) Clean up the substrate with ACE、IPA、D.I. water by ultrasonic

(2) Spin coating PMMA 495k

(3) Place the substrate and mold on stage

(4) Run thermal cycle

(5) Imprint

(6) Cooling down

(7) De-mold

(8) Observation with SEM、OM、AFM…etc

## 3-3-2 Fracture induced structuring
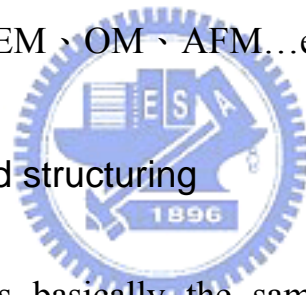
The process flow is basically the same with H-NIL , the only difference is that the mold of FIS is a blank substrate (ex. Si wafer).

## 3-3-3 UV-NIL fabrication process

The photo-polymerization polymer is chosen of PAK-01(PAK01 is an acryl resin which is mainly composed of tri-propylene-glycol-diacrylate monomer with dimethoxy-phenyl-acetophenone as a photo-initiator , Fig. 27) and SU-8 (epoxy resin). Process flow is shown below：

(1) Clean up the substrate with ACE、IPA、D.I. water by ultrasonic

(2) Spin coating with PAK-01 or SU-8

(3) Place the substrate and mold on stage

(4) Imprint

(5) Exposing with Xenon lamp (PEB for SU-8)

(6) De-mold

(7) Observation with SEM、OM、AFM...etc.

## 3-4 Anti-sticking layer

There are two available anti-sticking materials for our imprint processes. One is BA-m (polybenzoxazine) supplied from the lab. of prof. Chang（Department of applied chemistry，National Chiao Tung University），the other is commercial available dodecyltrichlorosilane (DDTS). BA-m is coated by a spin coater and is polymerized by heating. The DDTS is coated by liquid SAM，as shown in Fig. 28.

Process flow are shown below：

(1)BA-m coating

   (a) Spin coating

   (b) Heating 210℃ for 1~2 hour

(2) DDTS coating

   (a) Mix DDTS with toluene (DDTS：toluene＝1：100)

   (b) Dipping mold into solution for 60 minutes

## 3-5 Equipments and chemical lists

1. Electron Beam System，ELS-7500EX ELS，Elionix Corp.

(1) Department of Electrical Engineering , National Taiwan University

(2)Nano Science & Technology Center , National Chiao Tung University

2. E-Gun Evaporator , EBX-8C , ULVAC , Nano Science & Technology Center , National Chiao Tung University

3. RIE system , RIE-10N , SAMCO , Nano Facility Center , National Chiao Tung University

4. RIE system , HDP-RIE , 慶康科技 , Nano Facility Center , National Chiao Tung University

5. AFM , Dimension 3100 , Digital Instrument , Nano Science & Technology Center , National Chiao Tung University

6. Spin coater , 光映科技

7. Hot plate , Asone , digital hotplate HP-1LA

8. Mechanical pump , Alcatel , 2015SD

9. Air compressor , Silent-AIR , 30TC

10. Heating system , Arico , TC5E

11. Xe Lamp , Eurosep , BLC001

12. Water bath , Yihdern

13. Pneumatic system , Ashun

14. Chamber , 宇傑真空科技

15. Gauge , mini-convectron 275

16. ZEP-520A , ZEONREX Electronic Chemicals

(1)Thinner , ZEP-A , anisole

(2)Developer , ZED-N50 , n-amyl acetate

(3)Remover , ZDMAC , dimethylacetamide

17. PMMA 495k A4 , MicroChem

(1)Developer , MIBK：IPA

(2)Remover , Acetone

18. PAK-01-60 , Toyo Gosei co., LTD.

19. SU-8 2000.5 , MicroChem

(1)Thinner , cyclopentanone

(2)Developer , 1-methoxy-2-propanol acetate

(3)Remover PG

20. BA-m , dissolved in THF , Chang lab. of department of applied

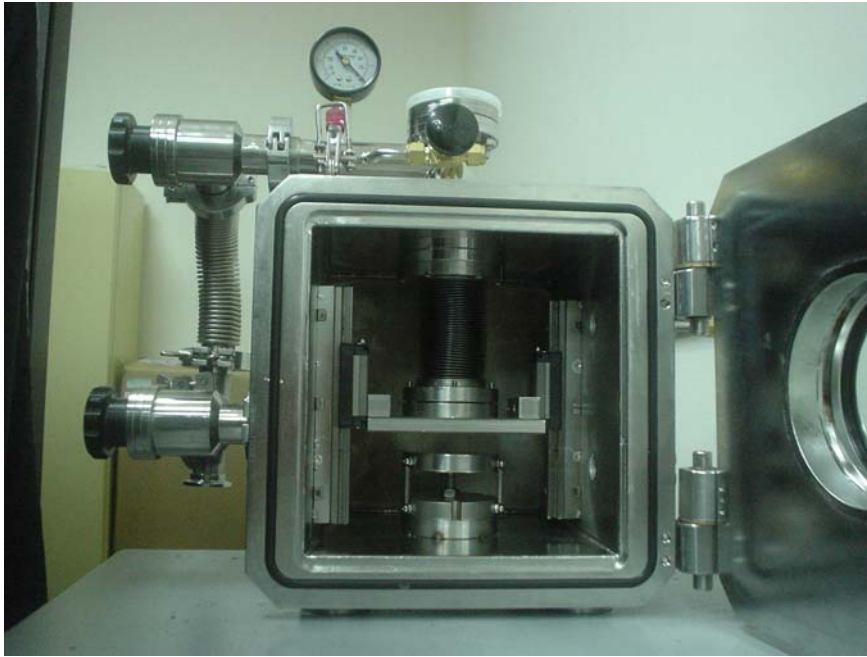chemistry , National Chiao Tung University

21. Dodecyltrichlorosilane (DDTS)

Fig. 15 The photograph shows the first model of our home-made nanoimprintor

(a) (b)
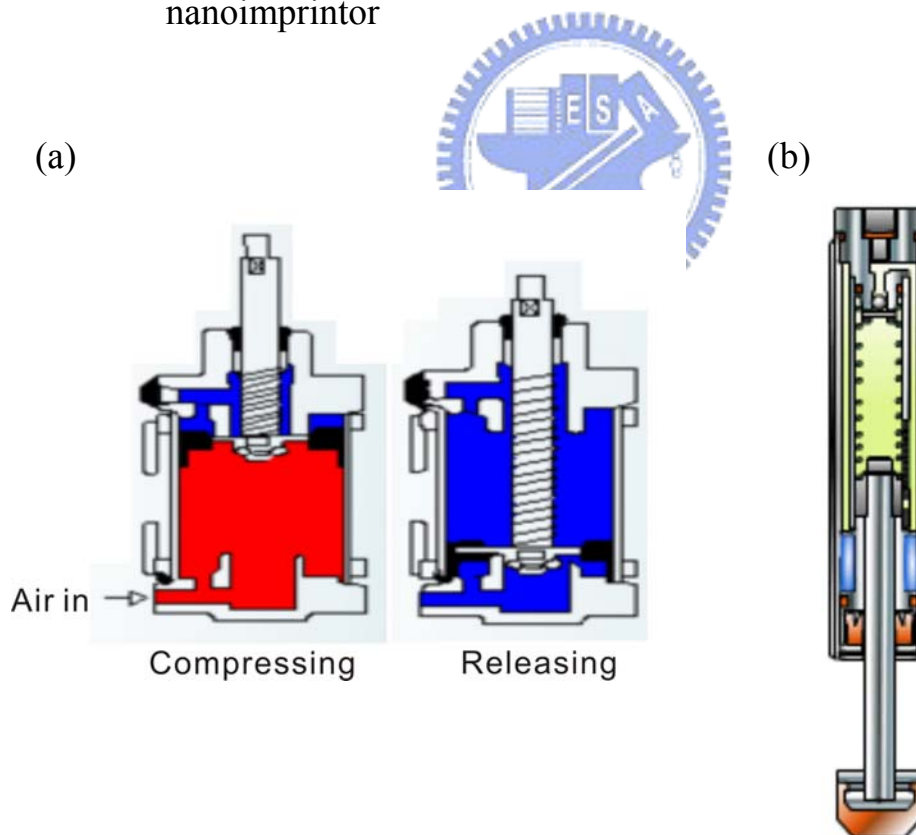


Air in →

Compressing        Releasing

Fig. 16 (a) The illustration shows the layout and process of pneumatic system (b) the layout of bumper
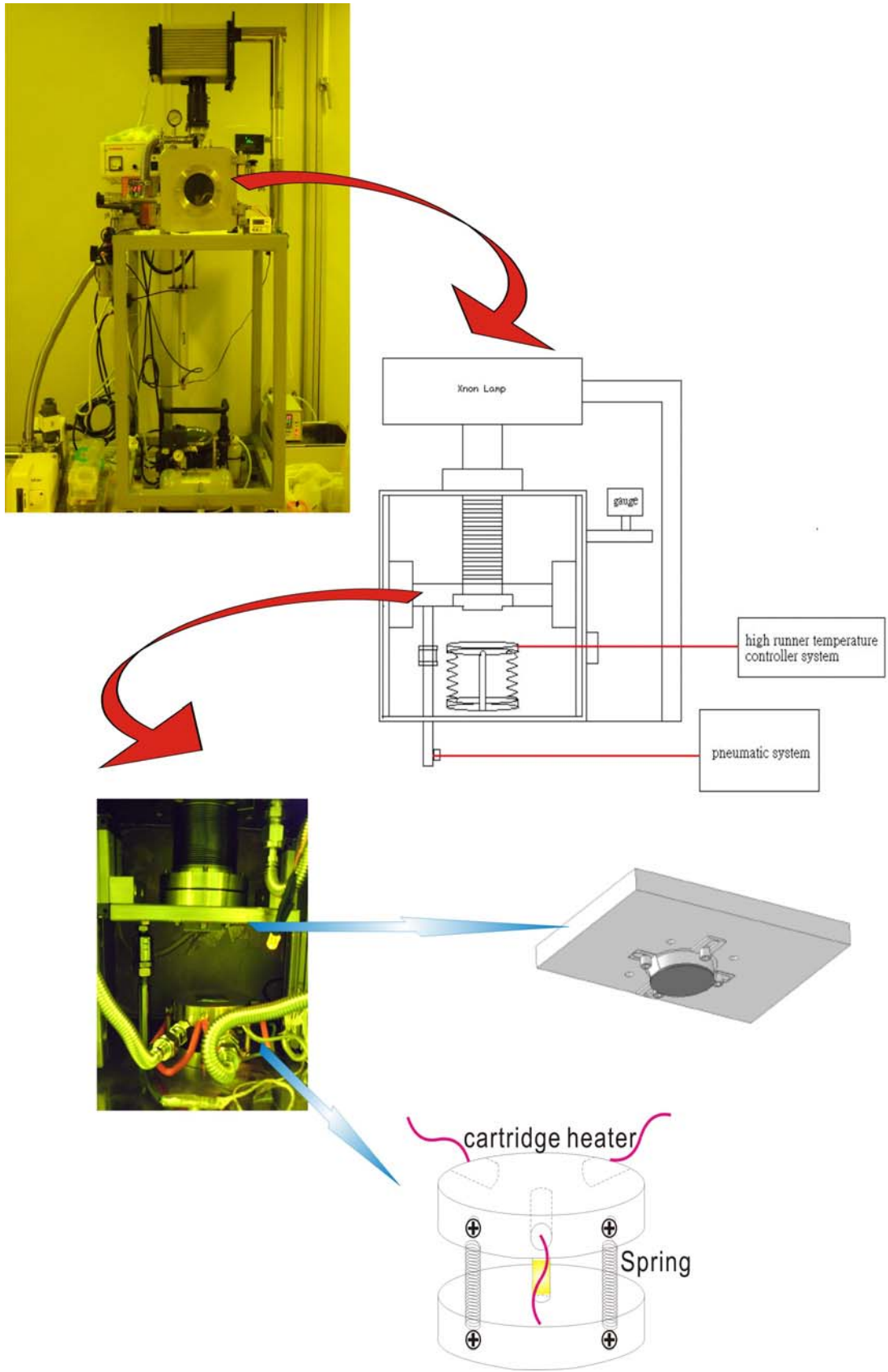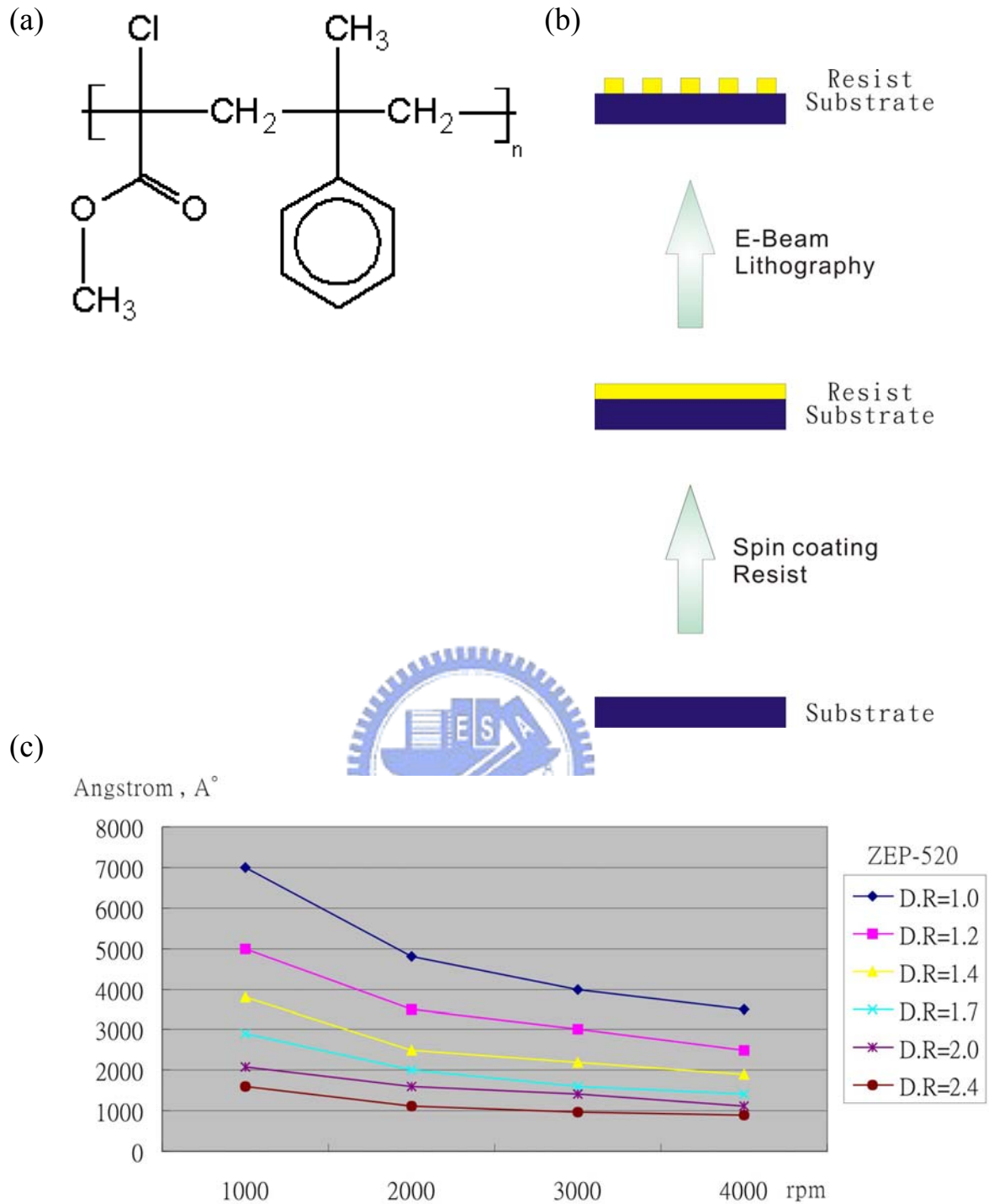
Fig. 17 The layout of our home-made nanoimprintor

Fig. 18 (a) The structure of ZEP-520 (b) the process flow of electron
beam lithography (c) the relative spin speed and film thickness of
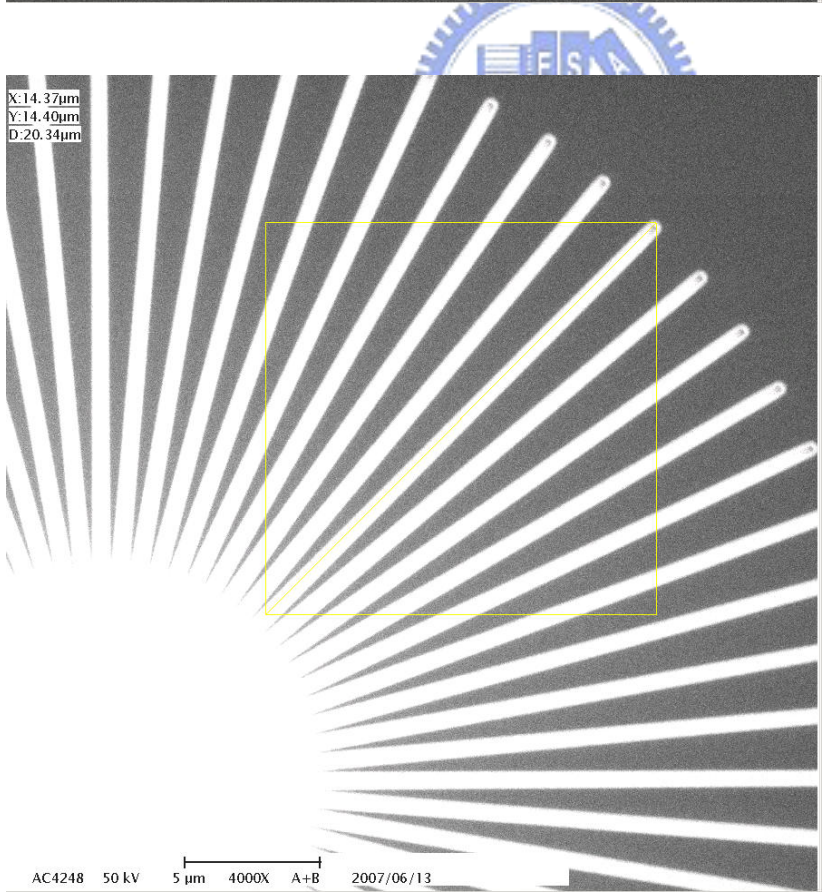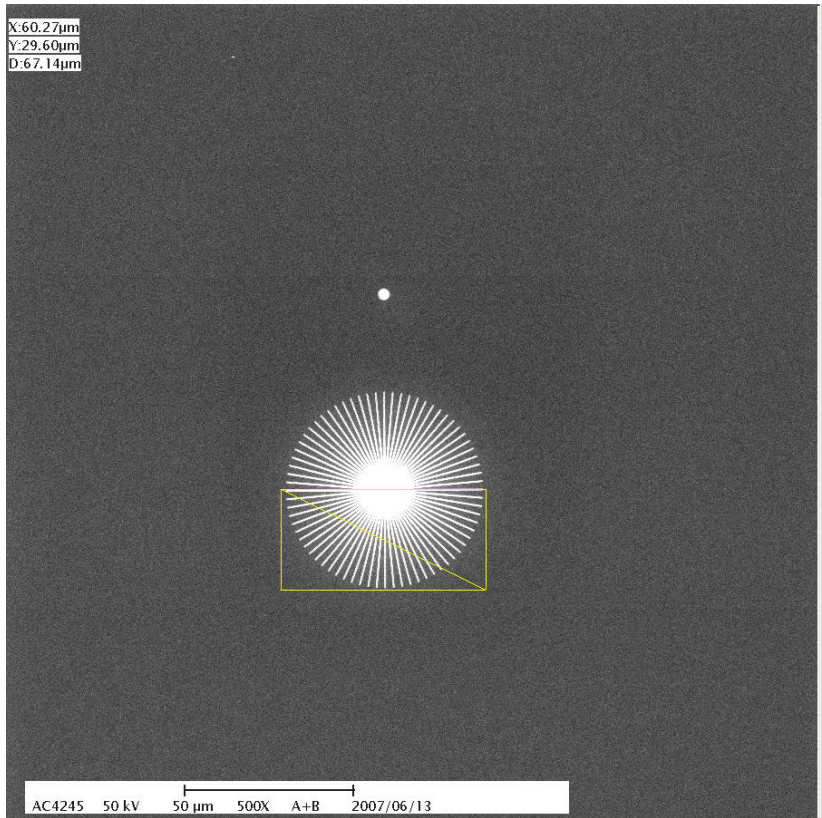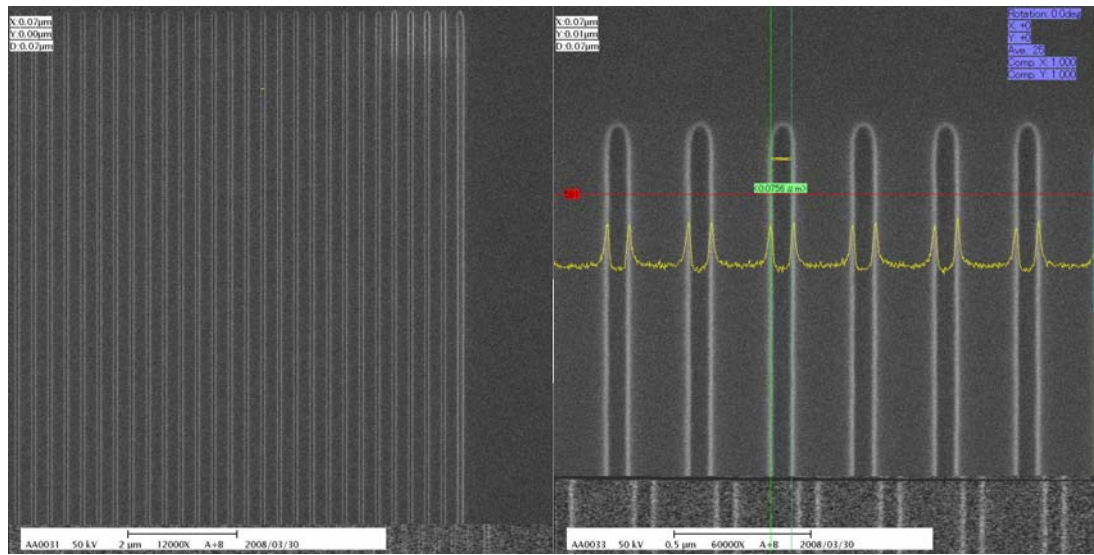ZEP-520A ( D.R = { Resist + Solvent } / Resist )

Fig. 19 The SEM image of star-like pattern after e-beam process , the

designed minimal size of each exposure line is 150 nm
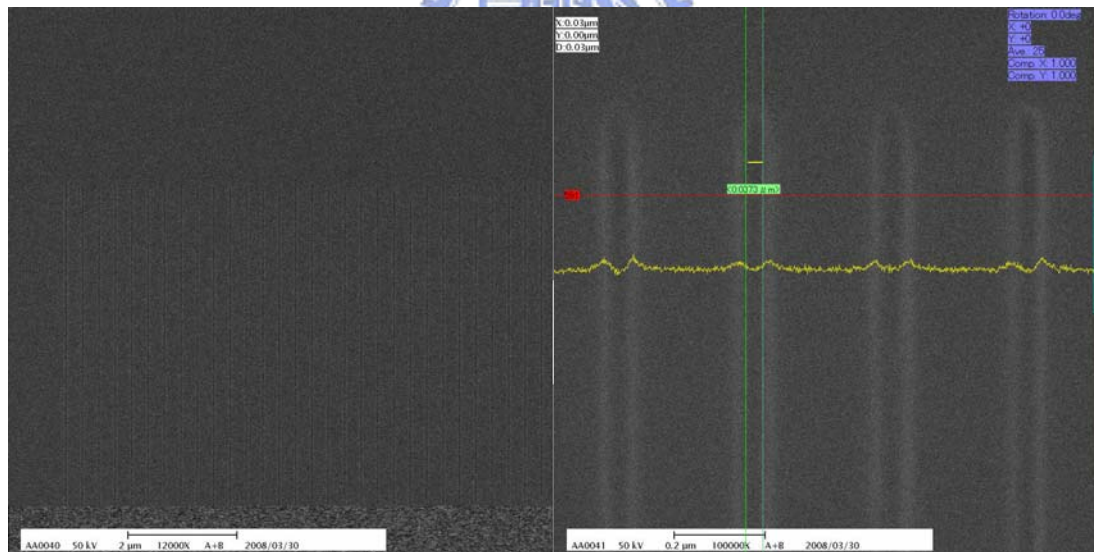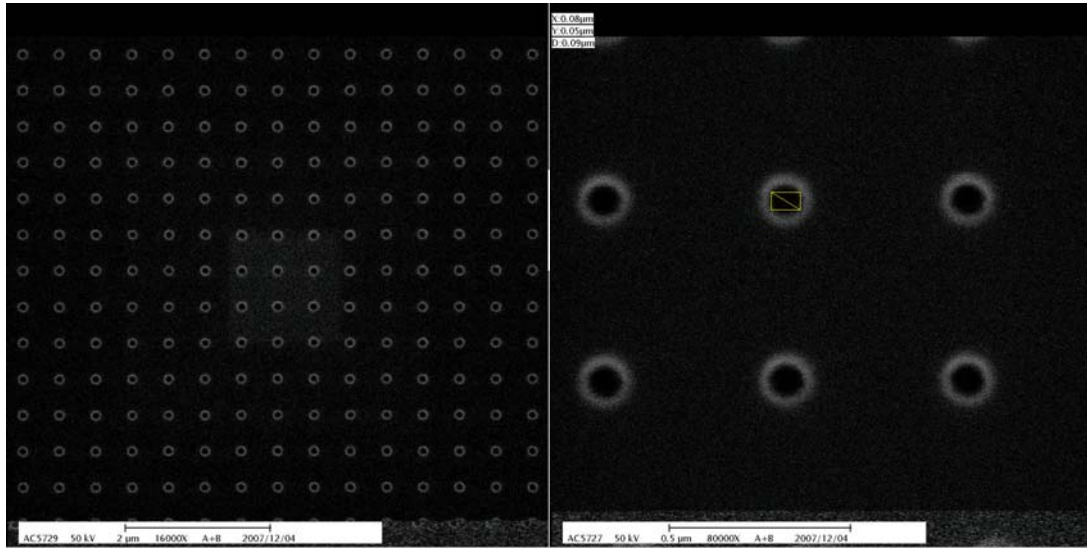
(a)



(b)



Fig. 20 The SEM image of grating after e-beam process , the designed

minimal size of each line is (a) 70 nm (b) 30 nm
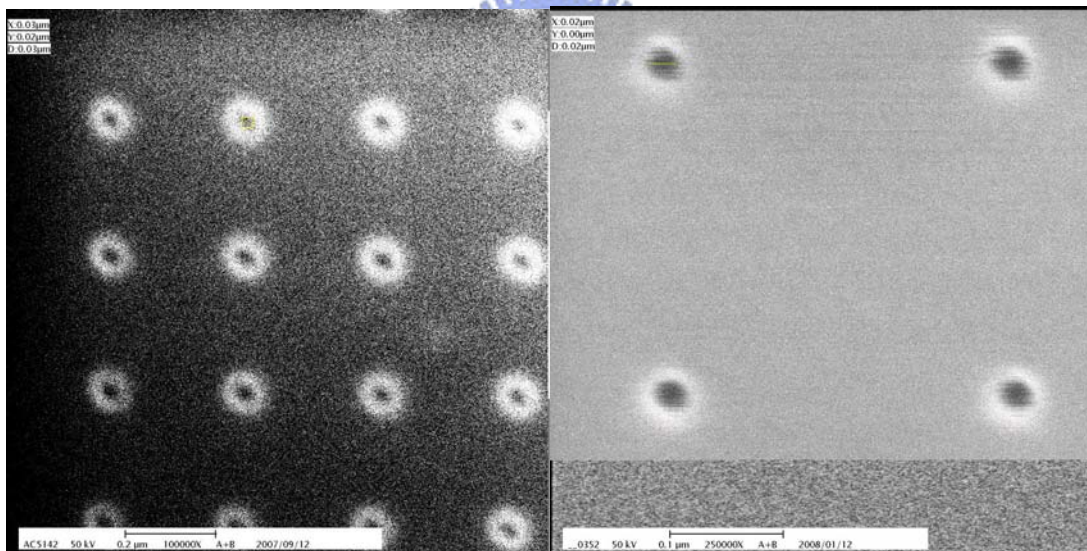
(a)



(b)



Fig. 21 The SEM image of hole array after e-beam process , the designed

minimal size of each hole is (a) 80 nm (b) 20 nm

Fig. 22 The SEM image of metal grating and hole array after lift-off

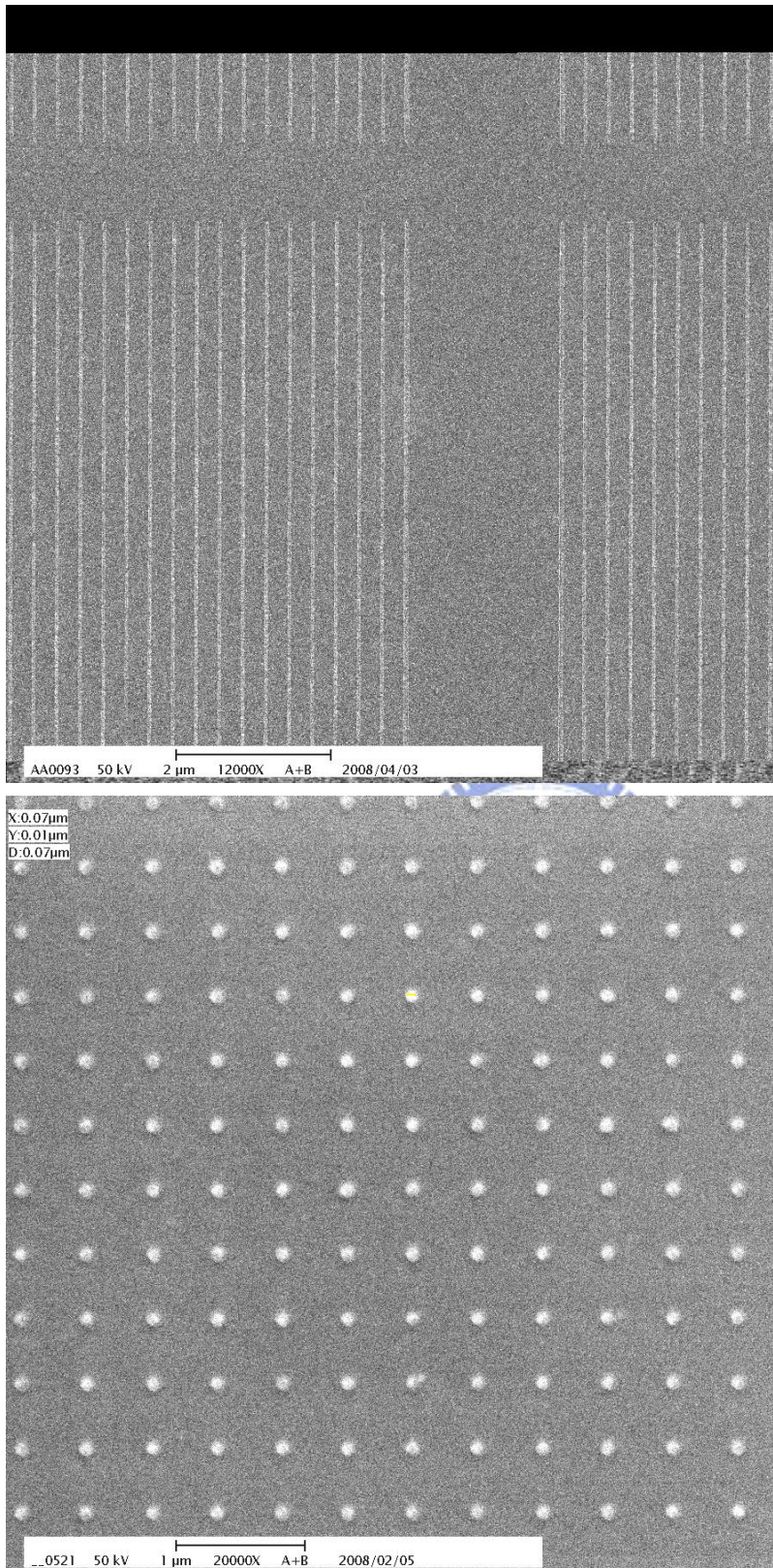process , the minimal size of (a) line 40 nm (b) hole 70nm
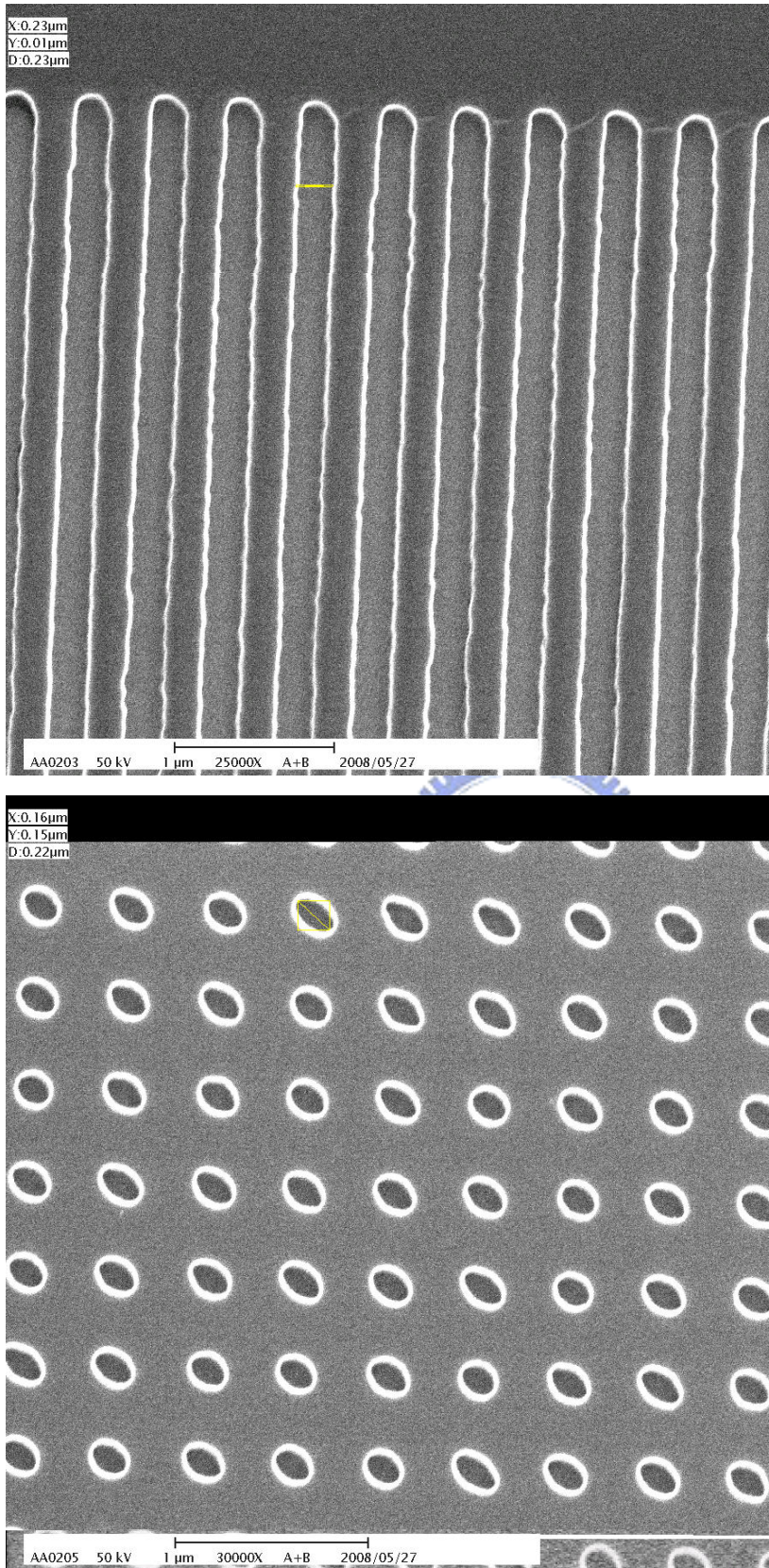
Fig. 23 The SEM image of grating and hole array after RIE process , the

minimal size of (a) line 230 nm (b) hole 160nm
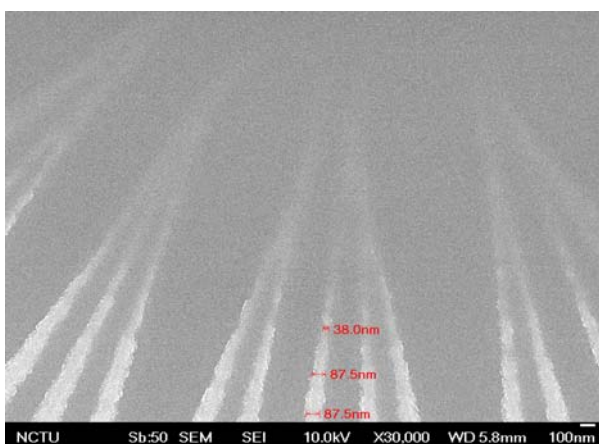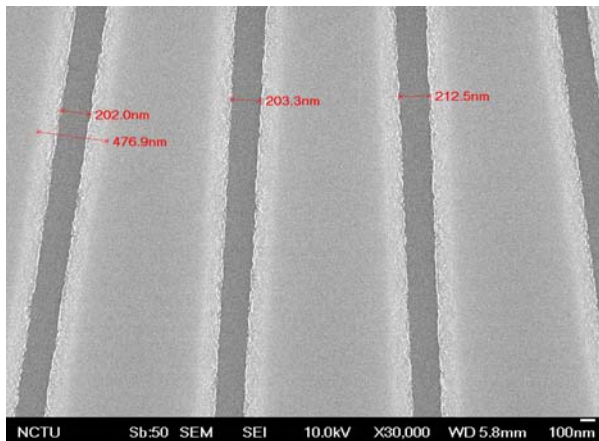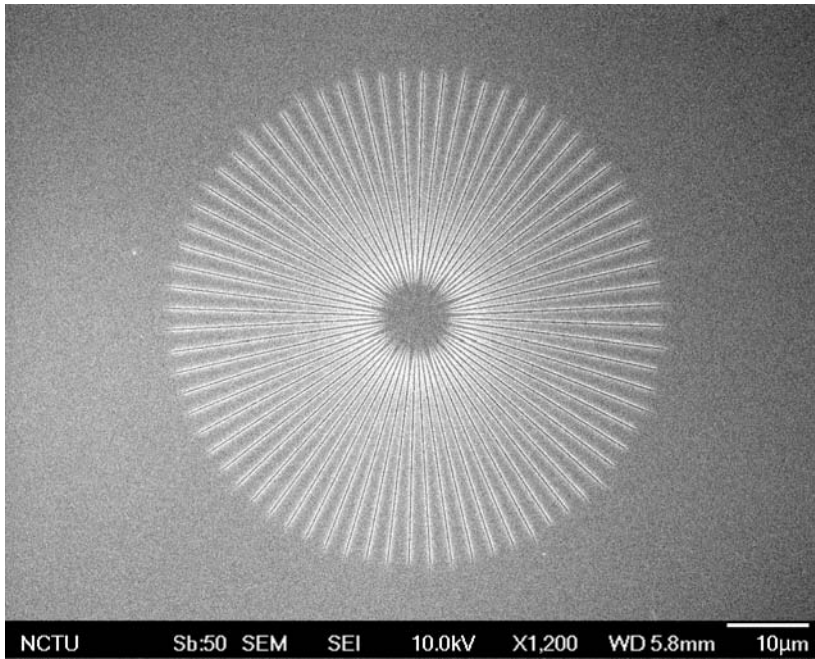
Fig. 24 The SEM image of star-like patterns after RIE process , the size

of each grating is about 200 nm
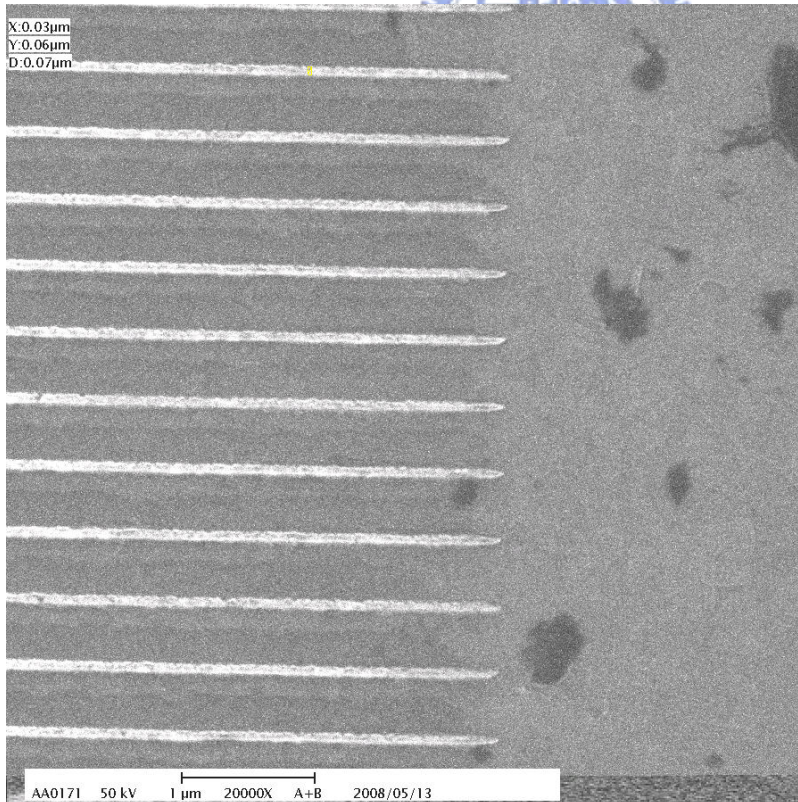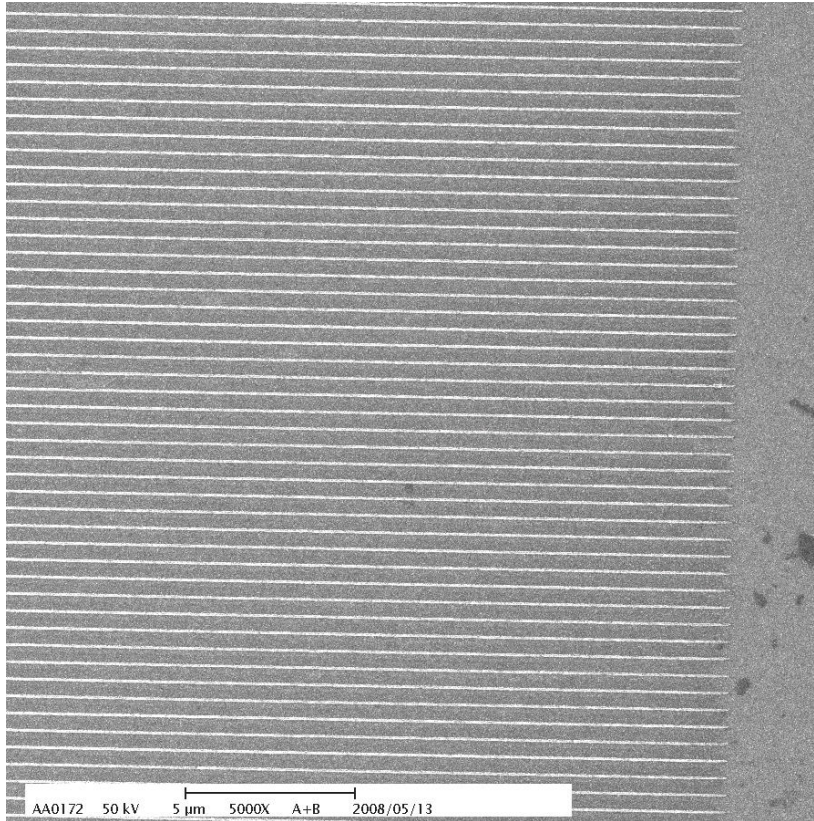
Fig. 25 The SEM image of grating on ITO substrate after lift-off process ,

the minimal size of each grating is about 60 nm
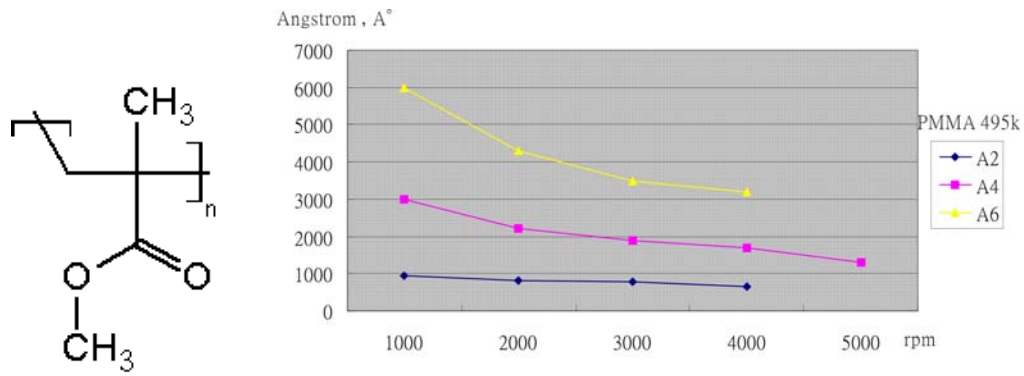
Fig. 26 The structure and spin speed vs. thickness diagram of PMMA

(a)

(b)

(c)
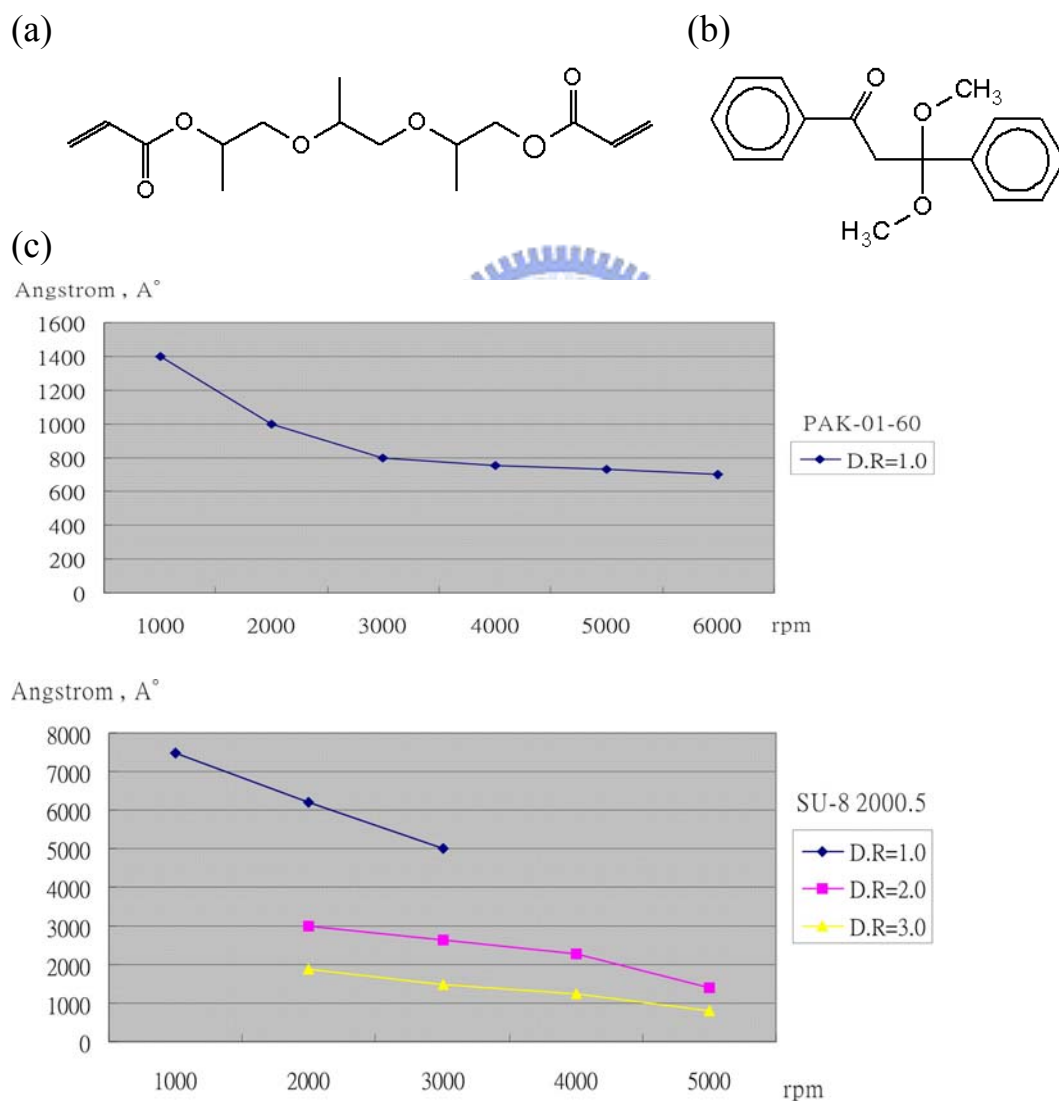


Fig. 27 The structure of (a) PAK-01 resist (b) PAK-01 photoinitiator (c) the spin speed

vs. thickness diagram of PAK-01-60 and SU-8 2000.5 resist

(a)



(b)
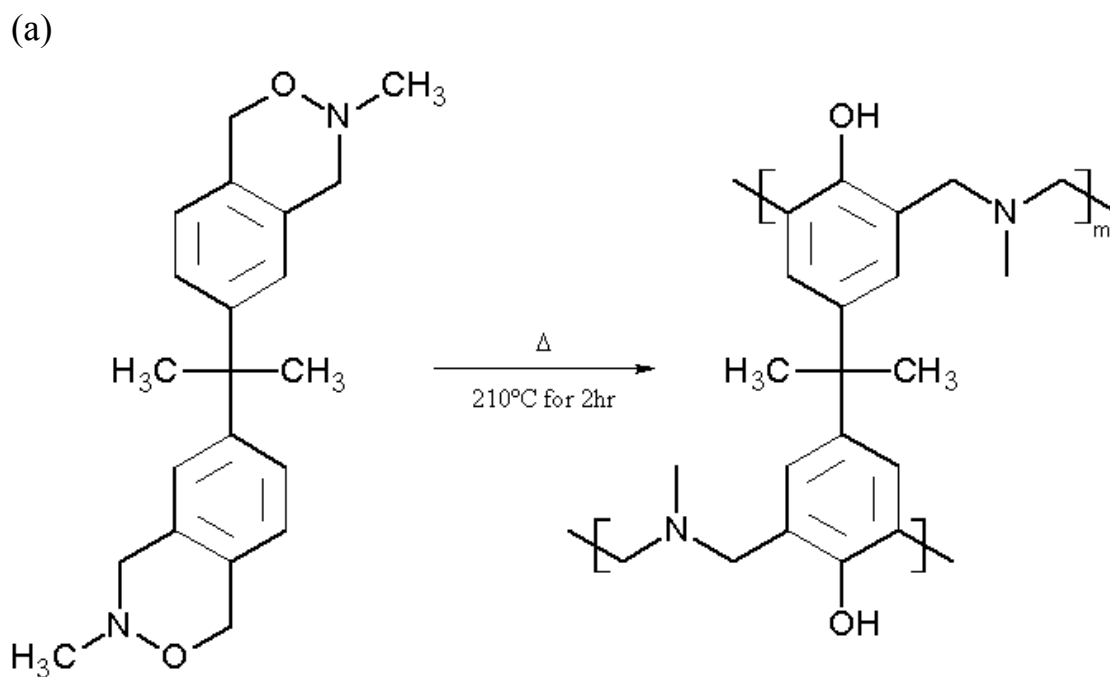
| Thickness | Tg | Contact angle ( ° ) | | | $\gamma$ |
|---|---|---|---|---|---|
| (nm) | (℃) | H$_2$O | EG | DIM | (mJ/m$^2$) |
| 449.3 | 179 | 112.1 | 91.7 | 81.7 | 16.7 |
| 79.3 | 180 | 111.7 | 91.6 | 81.3 | 16.9 |
| 13.5 | 174 | 112.8 | 93.1 | 82.0 | 16.5 |
| 11.8 | 176 | 112.3 | 93.0 | 82.3 | 16.3 |
| 8.8 | 178 | 113.1 | 92.8 | 82.8 | 16.2 |
| 6.3 | 176 | 112.7 | 93.3 | 82.5 | 16.2 |

(c)
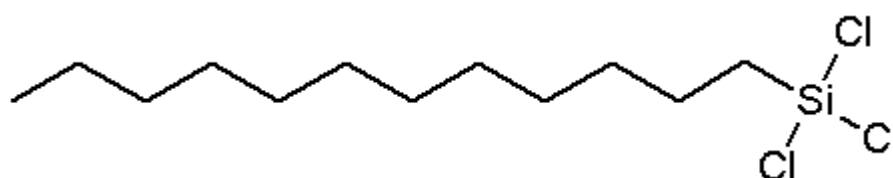


Fig. 28 (a)The illustration of the reaction of BA-m from benzoxazine (b)
the parameters of BA-m (c) the structure of dodecyltrichlorosilane
(DDTS)

# Chapter 4. Results and Discussion

## 4-1 Characterization of H-NIL nanoimprint results

The mold for our researches are usually fabricated by the e-beam and Lift-off process. However , the fringe of the metal hole array or star-like patterns are easily damaged and generated defects during the mold fabrication and imprint processes. Beside , they are not that easy to be characterized with SEM or AFM. Therefore , our researches are focused primarily on grating patterns.

## 4-1-1 H-NIL fabrication results

When we designed the layout of the mold patterns , we always put a larger marker nearby the desire patterns for the convenience of observation under SEM and AFM. However , there are many unexpected distorted line and bobbles nearby or inside the desire patterns after imprinting. After many tests , we found that these distort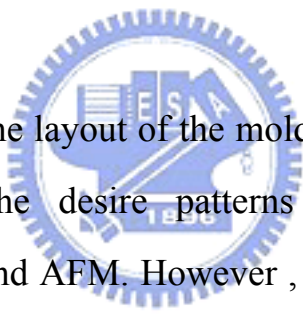ed patterns were caused by the marker pattern. Besides , their correlation will be redused when the desire patterns are far apart fromeach other (as shown in Fig.29). Therefore , we put the marker away from the desire patterns to avoid the correlation between the desire patterns and the marker. After that , we do obtain good H-NIL results with our home-made nanoimprintor , as shown in Fig. 30.

At the same time , the H-NIL mold are spin coated with BA-m thin film for the anti-sticking layer. The anti-sticking layer has served the purpose well for preventing the adhesion between resist and mold.

## 4-1-2 Fracture induced structuring results

During the investigation of H-NIL process , we uncovered some interesting phenomena. After some imprint tests with the same mold , there are some parallel patterns appear on some local area , as shown in Fig. 31(b). And this phenomenon became more clear when the mold was reused for several times , as shown in Fig. 31(c). We speculated that this phenomenon may resulted from the losing of anti-sticking layer (BA-m ~ 30nm) after a couple of tests. So , this results might be similar to Fracture induced structuring (FIS) results reported by Chou et.al in 2007[17].

On the other hand , when we peeled off the sandwich structure of two blank substrates within a PMMA polymer film , nano-scale grating patterns can be self-assembled. During these tests , we found two nanogratings with different pitch size on the sample. One is similar with Chou et al's experimental results with a grating period of $(4.0 \pm 0.6) * filmthickness$ , as shown in Fig.32 ; the other has a pitch size larger than the previous one , as shown in Fig.33.

The patterns which was shown in Fig. 32 is more clear and uniform when thicker resist film was applied. Such nanogratings are generally found in around few $cm^2$ area. In summary , the phenomenon of FIS is resulted from the facture of polymer (or crack propagation of polymer) , as shown in Fig.34 ; the nanogratings fabricated with this method is easier than any other fabrication process. However , we must peel off the sample very carefully. The uneven peeling force (or mixed fracture modes) will greatly affect the results.

On the other hand , the other nanogratings shown as Fig. 33 are generally dispersed on local breaking edge. Besides , these structures were distorted along the breaking edge and the grating direction of each different block are usually different. We concluded that the results come from the uneven peeling force because the sample was peeled off manually.

## 4-2 Characterization of UV-NIL nanoimprint results

The UV-NIL was proceeded with two different UV curing resist , one is the PAK-01-60 , the other is SU-8-2000.5. In the beginning of our experiment , we tried UV-NIL with PAK-01-60. It is a high resolution、low adhesive UV-NIL resist. However , we can only get poor results with this resist. Therefore , we tested with SU-8 resist. Unfortunately , we still can not get good UV-NIL result. Both results show that the depth is around 10~20 nm which is less than the depth of the metal grating (~80 nm) on the mold. On the other hand , we tried UV-NIL processes with different half-pitch size grating (250 nm and 70 nm Al metal grating , as shown in Fig. 35) patterned mold and different thickness of UV resist , but we all get similar results. The gratings have round shape instead of vertical edge. The only difference between them is that the smaller metal grating patterned mold produces a rougher surface , as shown in Fig. 36~38. Therefore , we conclude that it is due to insufficient mechanical force , the illustration is as shown in Fig. 39.

In general ,   the mechanical force applied on UV-NIL should be

lower than H-NIL. However , when we proceed UV-NIL processes with our home-made nanoimprintor , the imprint force was exercised in max. pressure (0.7 MPa , larger than 0.4MPa of H-NIL process) , but it is still not enough for pressing the mold to reach the bottom.
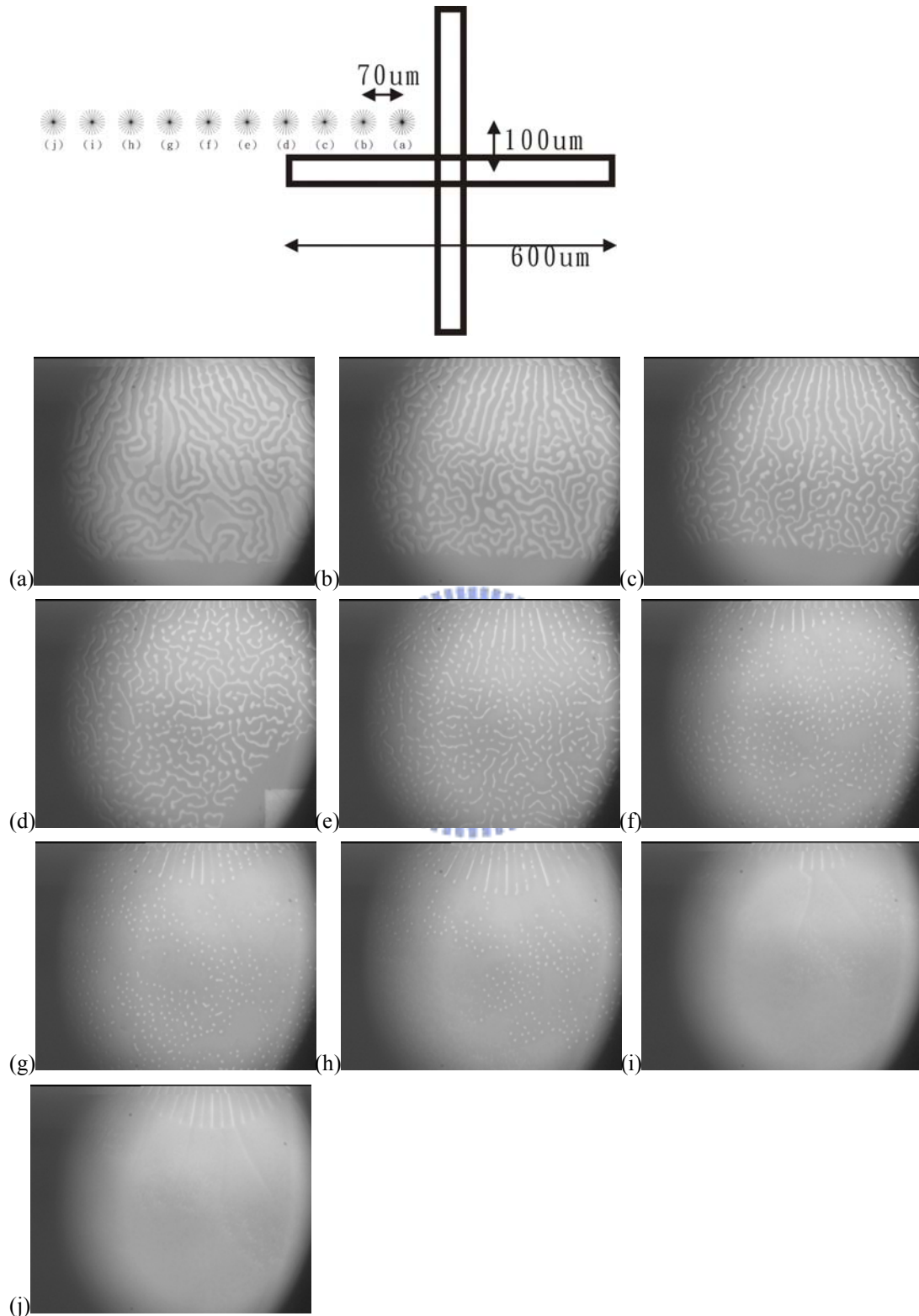
Fig. 29 The geometric patterns between the star-like pattern and marker
(a)~(j) represent the distance far away from marker , and (a) is the
closest to marker.

(a)
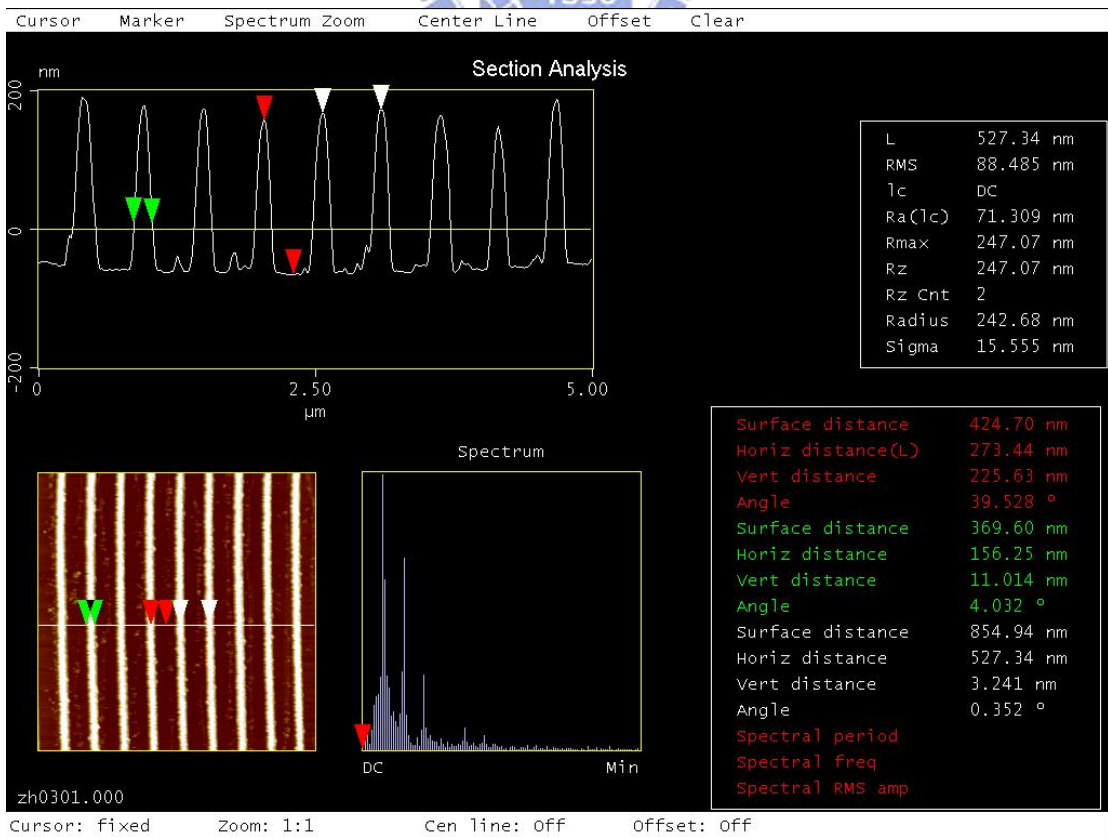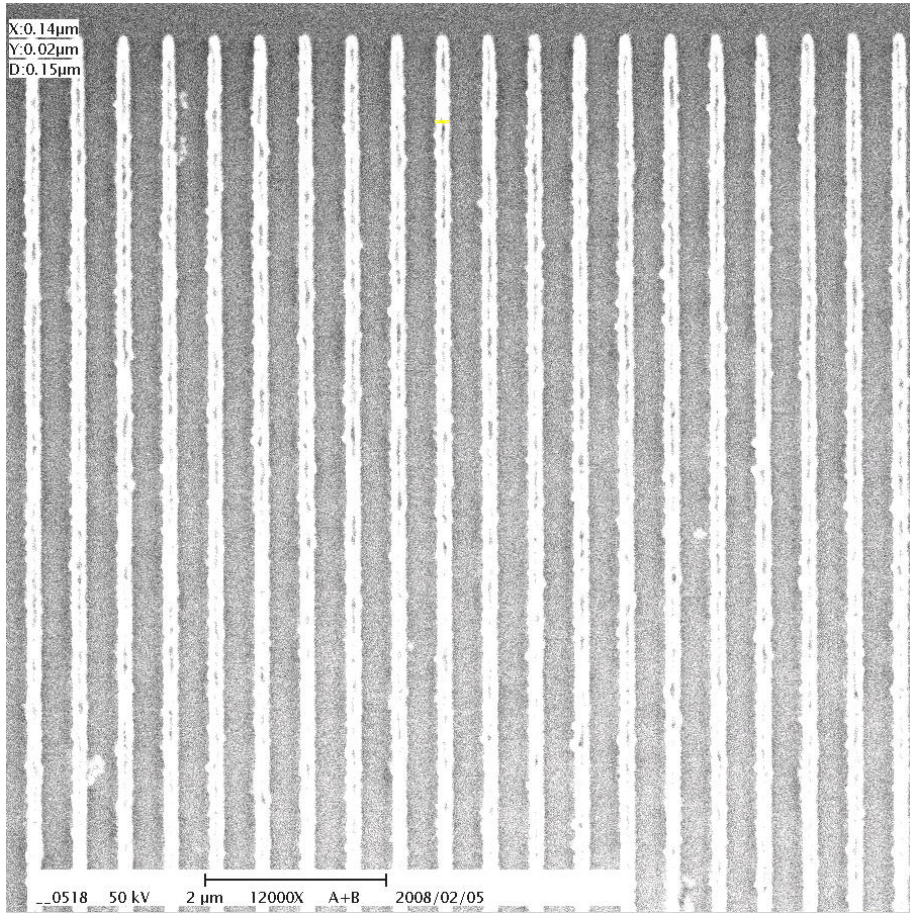
(b)
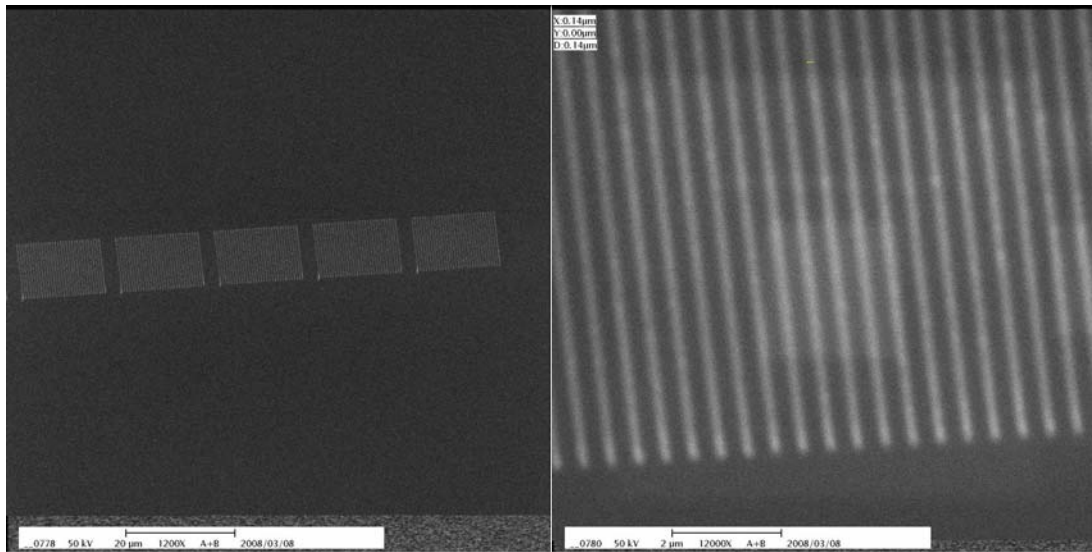


(c)
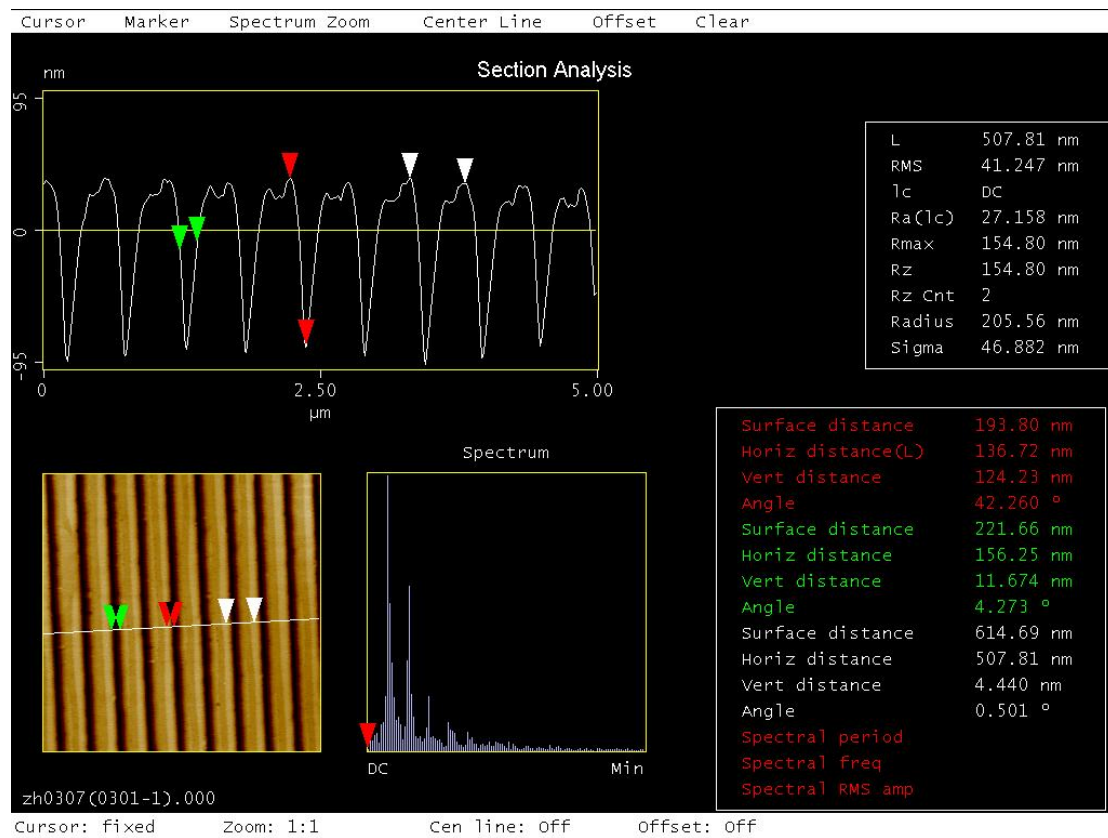


Fig. 30 (a) The SEM and AFM image of the Si mold (b) the SEM images
of imprint results (c) the AFM image of the imprint data

(a)
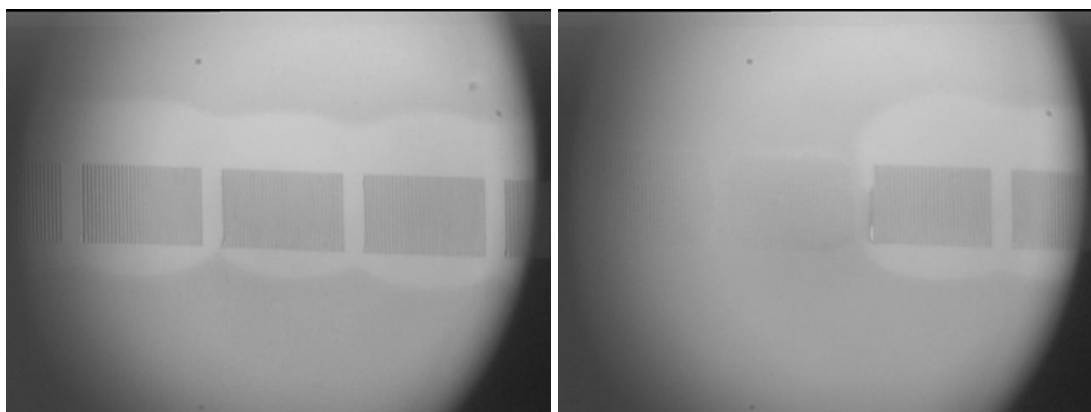


(b)
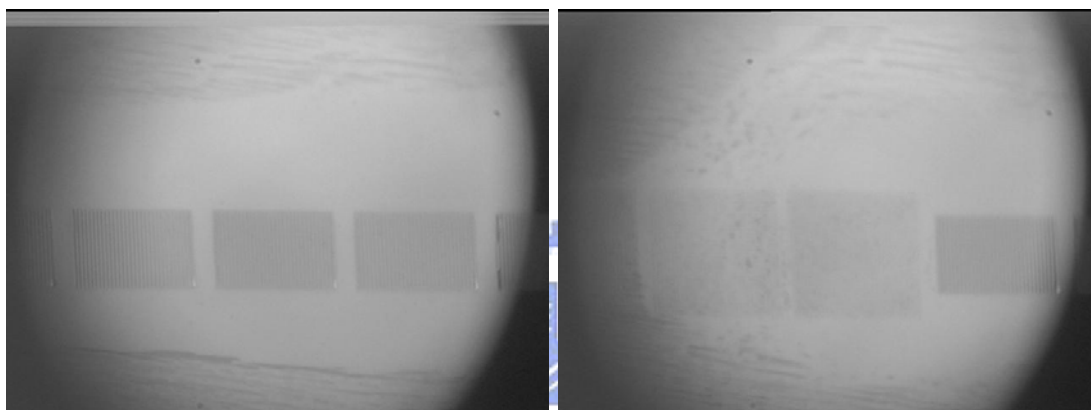


(c)



Fig. 31 (a) These images represents the first imprint (b) the images after

three imprinting (c) this image shows the parallel structures

beyond the desirably patterns after further imprinting

(a)



(b)
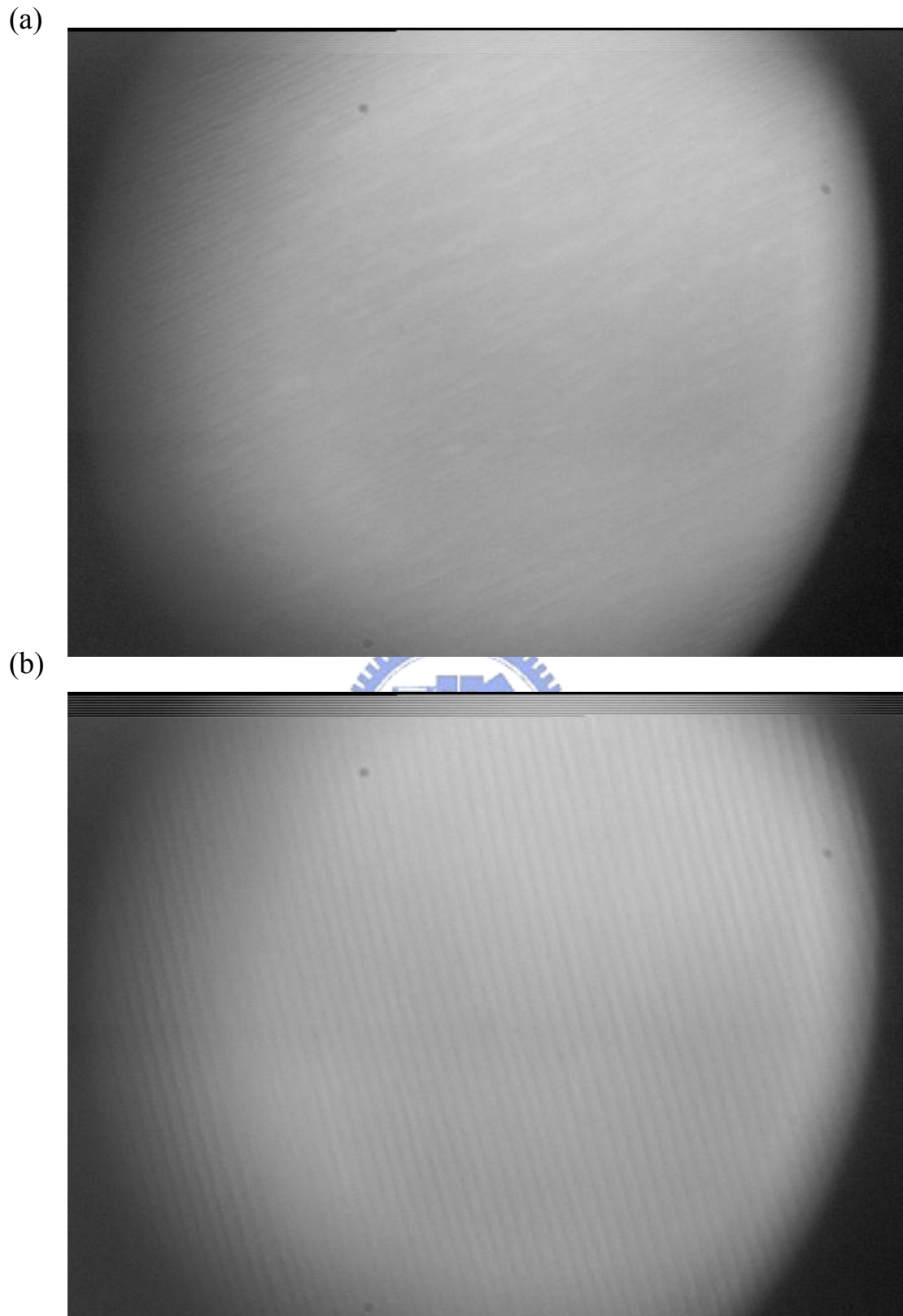


Fig. 32 (a) The FIS by peeling from 130 nm thick PMMA film (b) The

FIS by peeling from 300 nm thick PMMA film
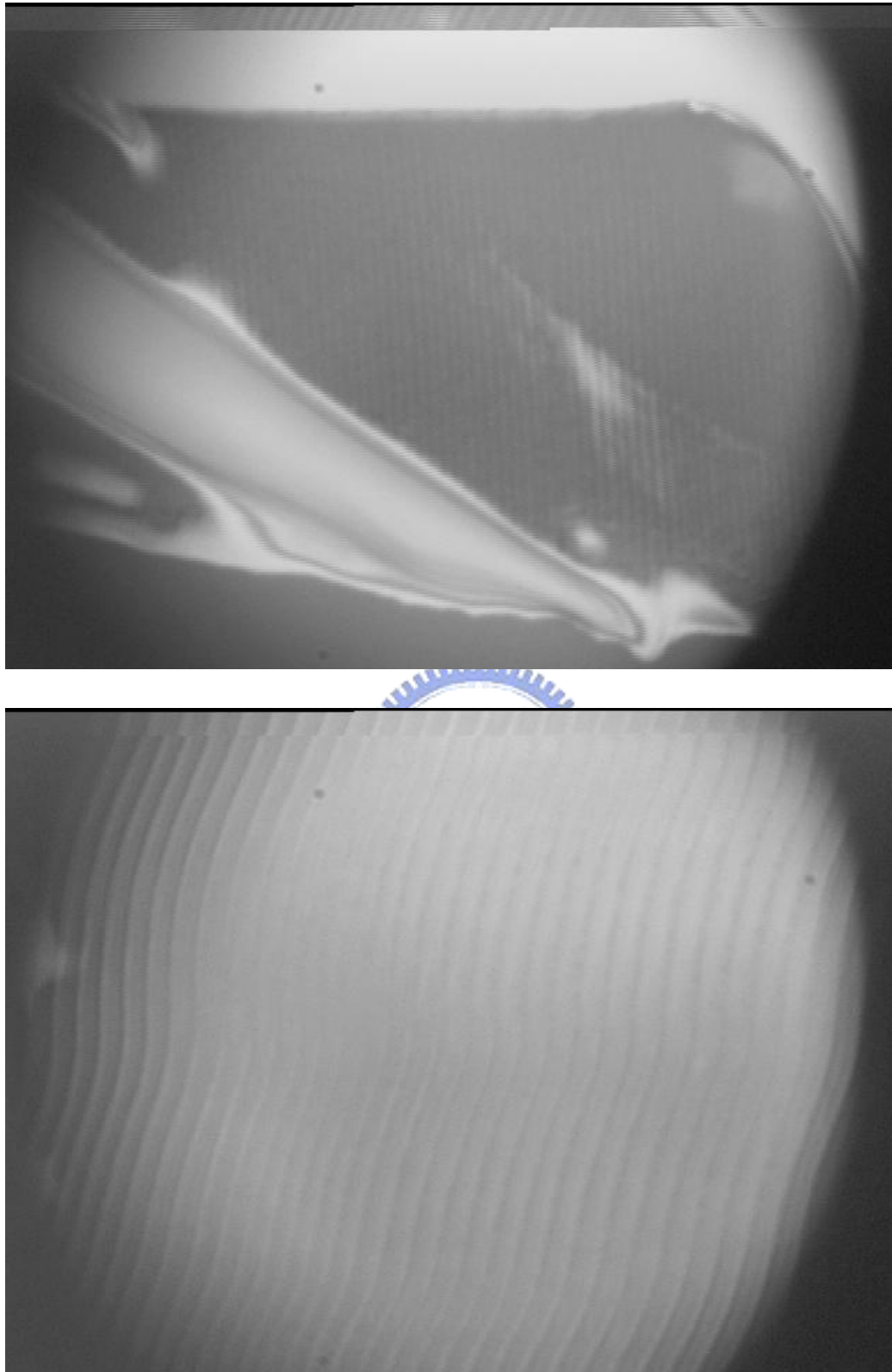
Fig. 33 The structures appear near the breaking edge by peeling from 130

nm thick PMMA film on the same sample

(a)

Opening (Mode I, $K_I$)

Tearing (Mode III, $K_{III}$)

Sliding (Mode II, $K_{II}$)

(b)

Applied Tensile Stress

Undeformed Elastic Material

Directions of Craze Growth

Advancing Crack

Craze

Craze/Bulk Interface

Undeformed Elastic Material

Craze Tip (Dugdale-like)
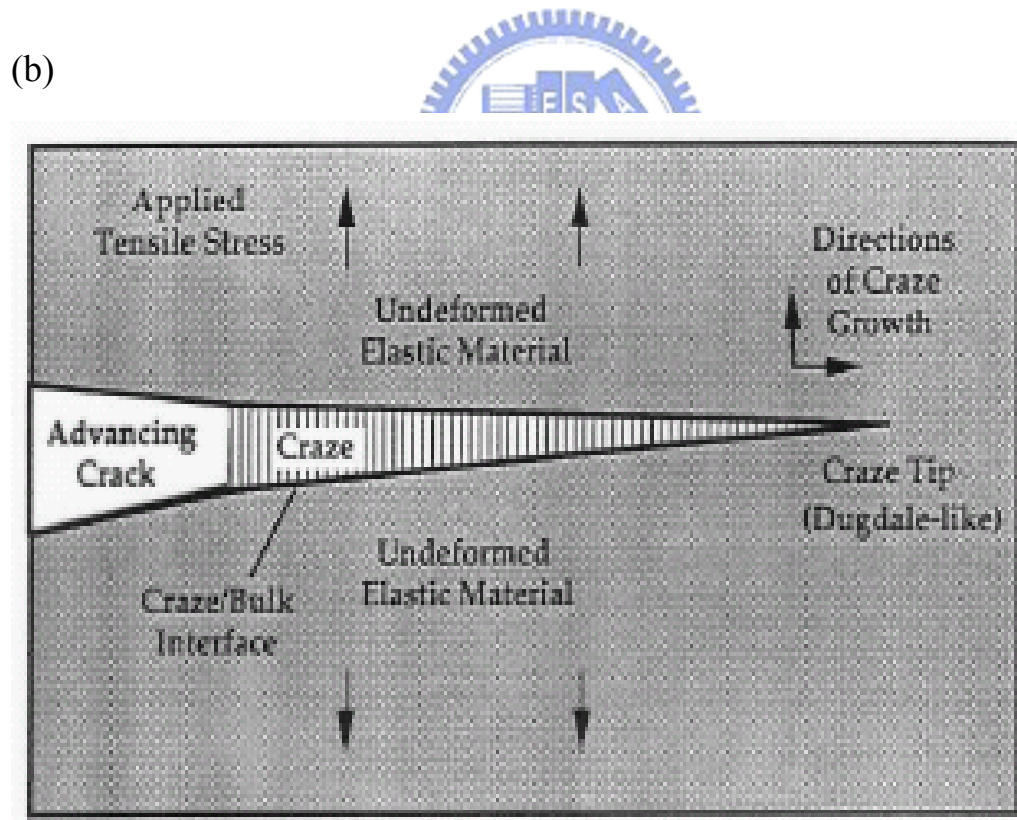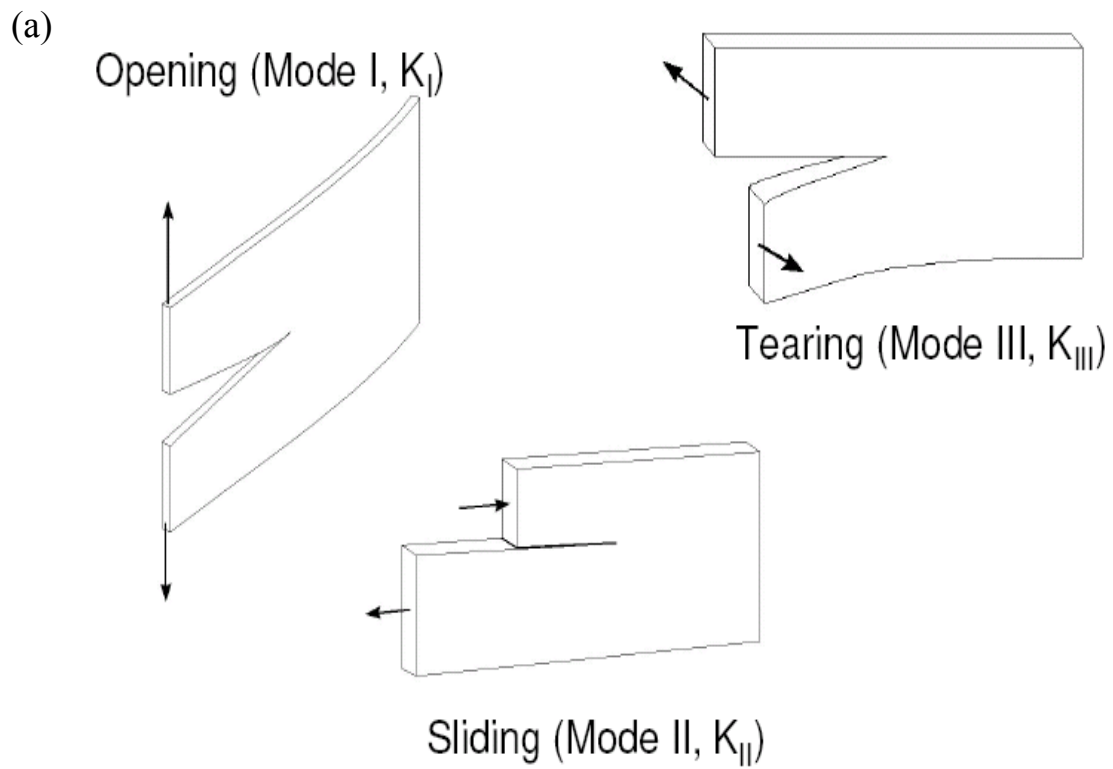
Fig. 34 (a) The basic three modes of fracture (b) the illustration of fracture induced structuring with polymer resist thin film
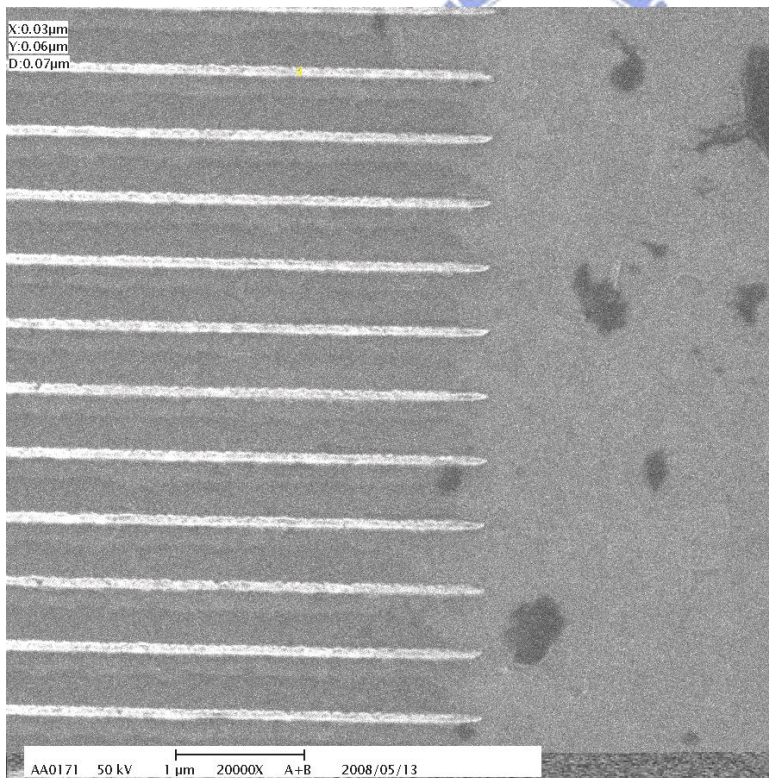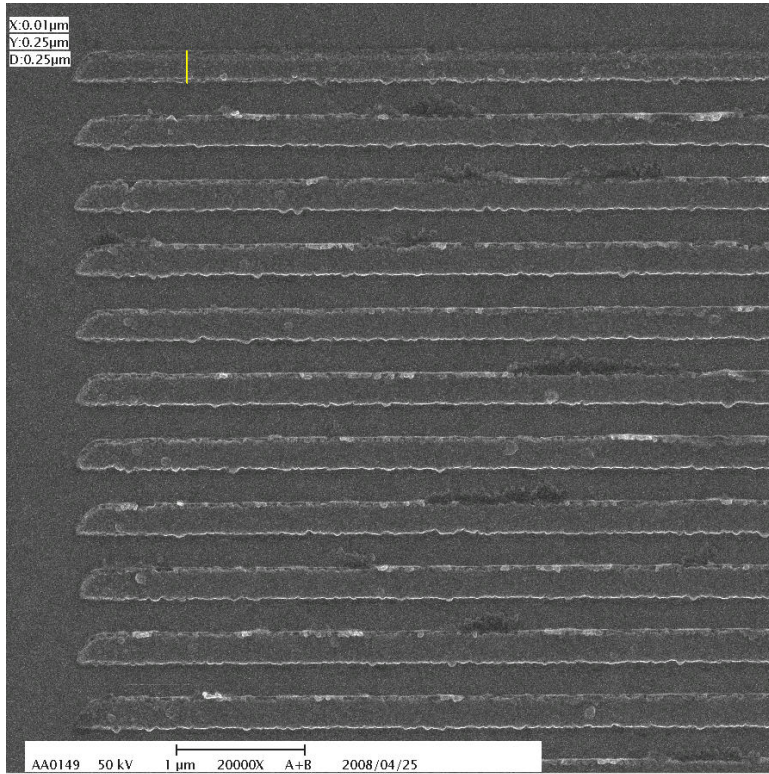
Fig. 35 The SEM images of the ITO patterned mold (a) is the 250 nm
metal grating (b) is the 70 nm metal grating
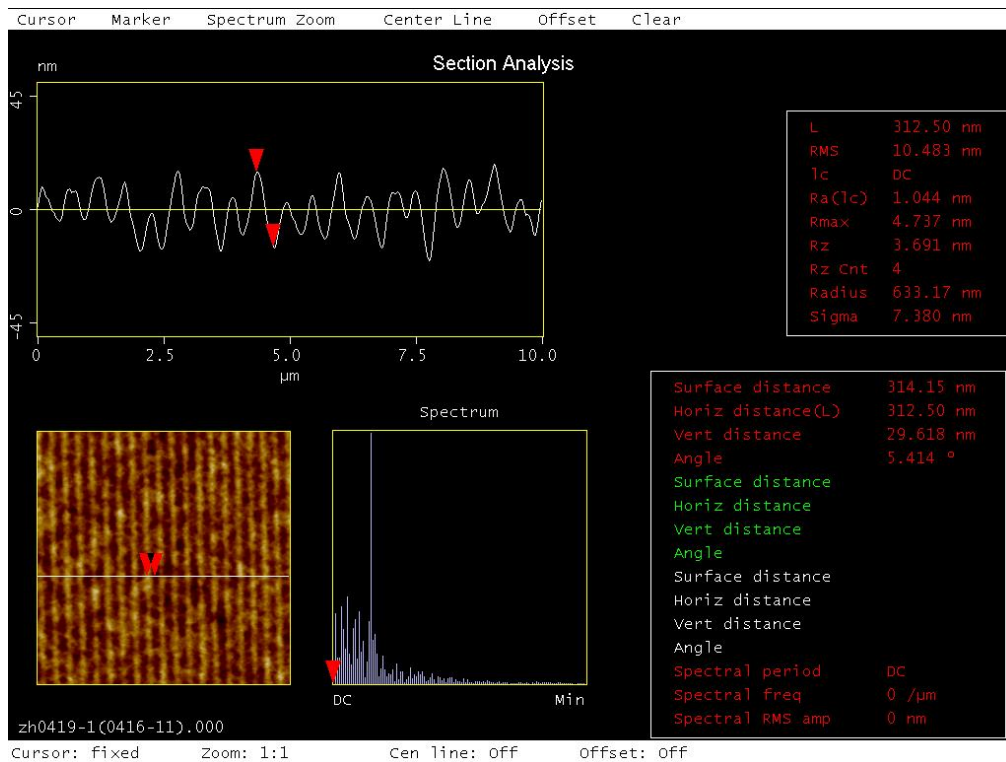
Fig .36 The result of UV-NIL with PAK-01-60 resist and 250 nm metal
grating patterned mold
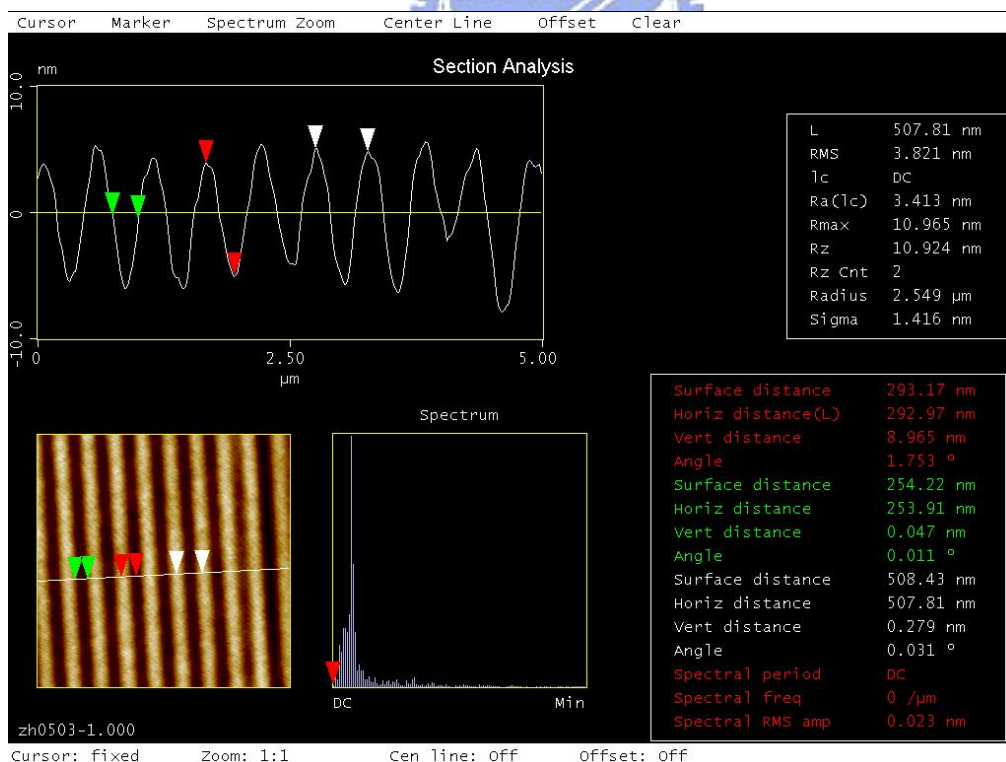


Fig .37 The result of UV-NIL with SU-8 resist and 250 nm metal grating
patterned mold
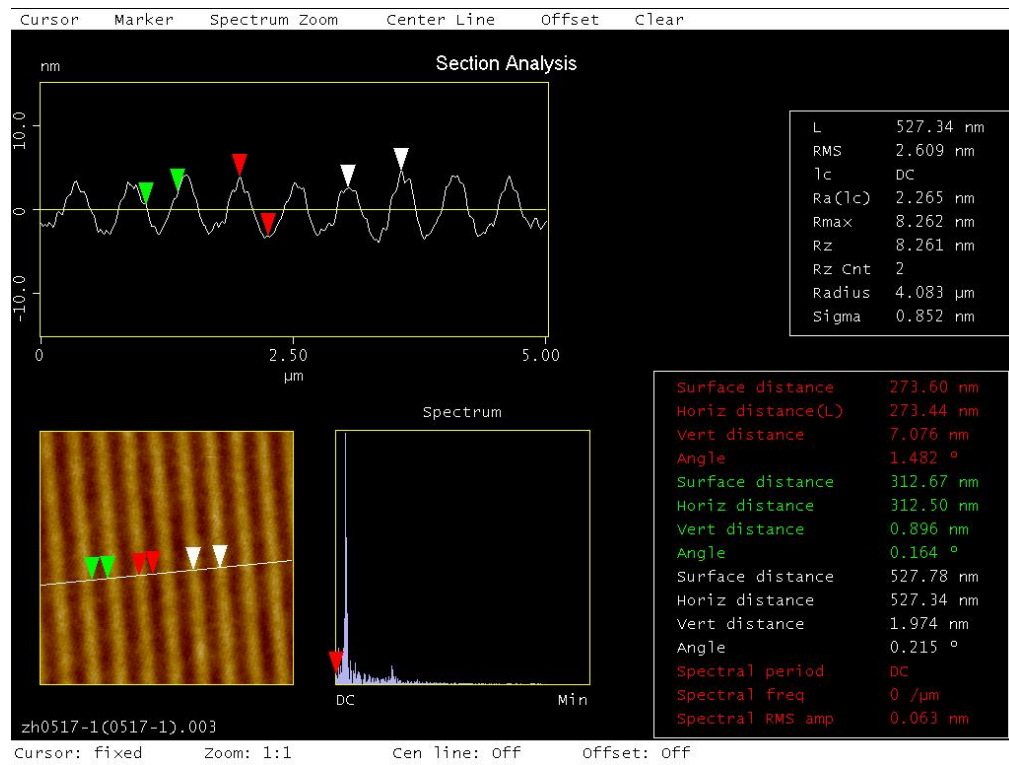
Fig. 38 The result of UV-NIL with SU-8 resist and 70 nm metal grating

patterned mold
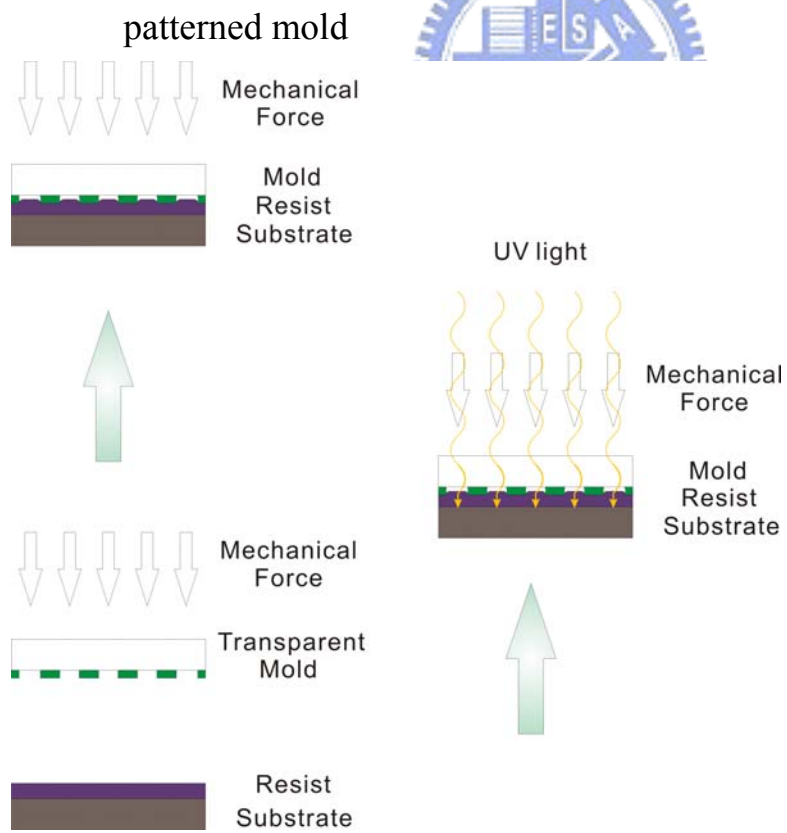


Fig. 39 The illustration shows the UV-NIL process with the insufficient

imprinting force

# Chapter 5. Conslusion

## 5-1 Improvement of NIL techniques

In summary , we built up a home-made nanoimprint tool that can work both in H-NIL and UV-NIL modes. We can fabricate any patterns on Si or transparent ITO、quartz substrate by combing the nanoimprintor with e-beam lithography technology. Therefore , we can applied our techniques on other nano researches , such as solar cell、photonics、bio-senser…etc..

The uniformity of imprinting force is one of our concern in our home-made equipment. In our imprinting results , the available area of H-NIL results are centralized , at least 50% of the area shows good pattern uniformity , as shown in Fig.40(1). However , we can't control the imprinting results of the edges. This phenomenon is similar with the other commercial bonding nanoimprint systems[22]. The uniformity of the edge on the sample is usually not well-controlled during the imprinting process. This problem seems happened in all those systems using pneumatic system to provide the imprint force.

We counted the defects between the middle and periphery of the patterns. From the results , we conclude that the defects are easily generated in the periphery of the patterns , however , the middle of the imprinting patterns have less defect (Fig.40). On the other hand , the UV-NIL results are generally more uniform and no apparent defects are generated during the imprinting process. The uniformity of our home-made nanoimprintor is good for the simple imprinting.

During the research of the H-NIL processes with our home-made nanoimprintor , we uncovered some interesting results which we attributed to the FIS. The phenomenon is conclusively resulted from the facture of polymer. This process has the potential application for the fabrication of large-area nanograting patterns.

On the other hand , the result for UV-NIL is satisfied because of he insufficient imprint force of our home-made nanoimprintor. With more efforts , we should be able to improve our pneumatic system to make this process more controllable.

## 5-2 Future goal on solar cell

As the increasing needs for green energy , people now pay more and more attention on solar energy because it is the most important source of regenerative energy and represents mankind's only inexhaustible energy source. However , most of the solar cells (Table3) require large areas and high ordered structures inside the modules to improve the conversion efficiency. There are a lot of groups investigated in fabricating large-area anti-reflection layer on Si wafer with nanoimprint technique[23][24][25]. Most of the researches presented good anti-reflection properties with these imprinted polymer layers. However , there is no report on the fabrication of the real P-N solar cell devices with nanoimprint technique , nor tests of the properties of the solar cell device. Therefore , we can dedicated this method to the solar cell applications.

Among all of the conventional lithography technique , NIL technology has the potential for the nano-scale duplication and the

process that is relatively inexpensive and easy. With further improvement ,
we can combine this techniques with solar cell devices and provide a
promising technique for the fabrication of high efficiency solar cell.

(1)
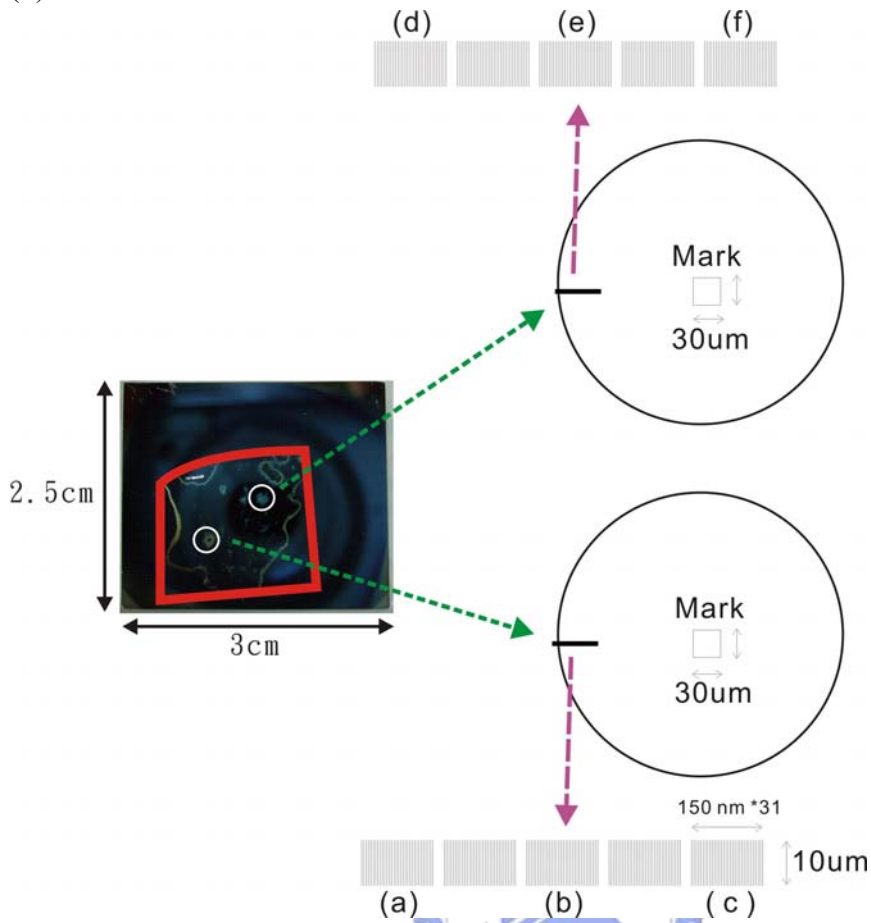


(2)(a)
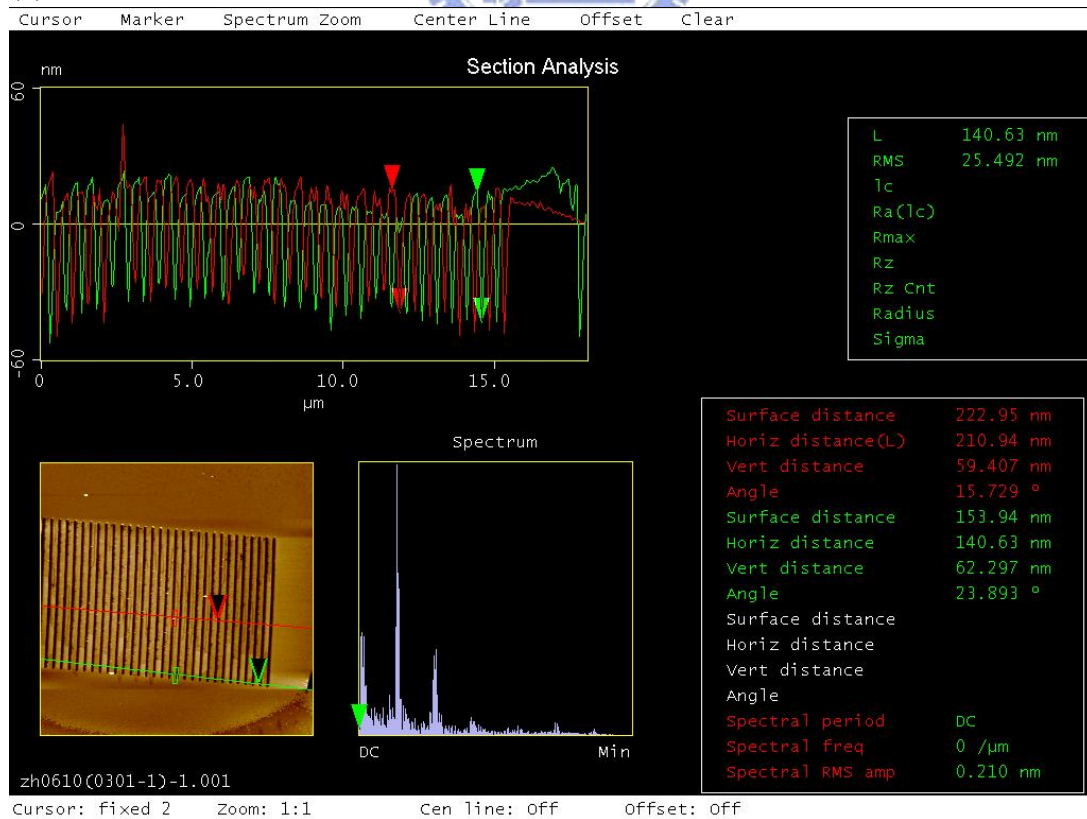
(b)
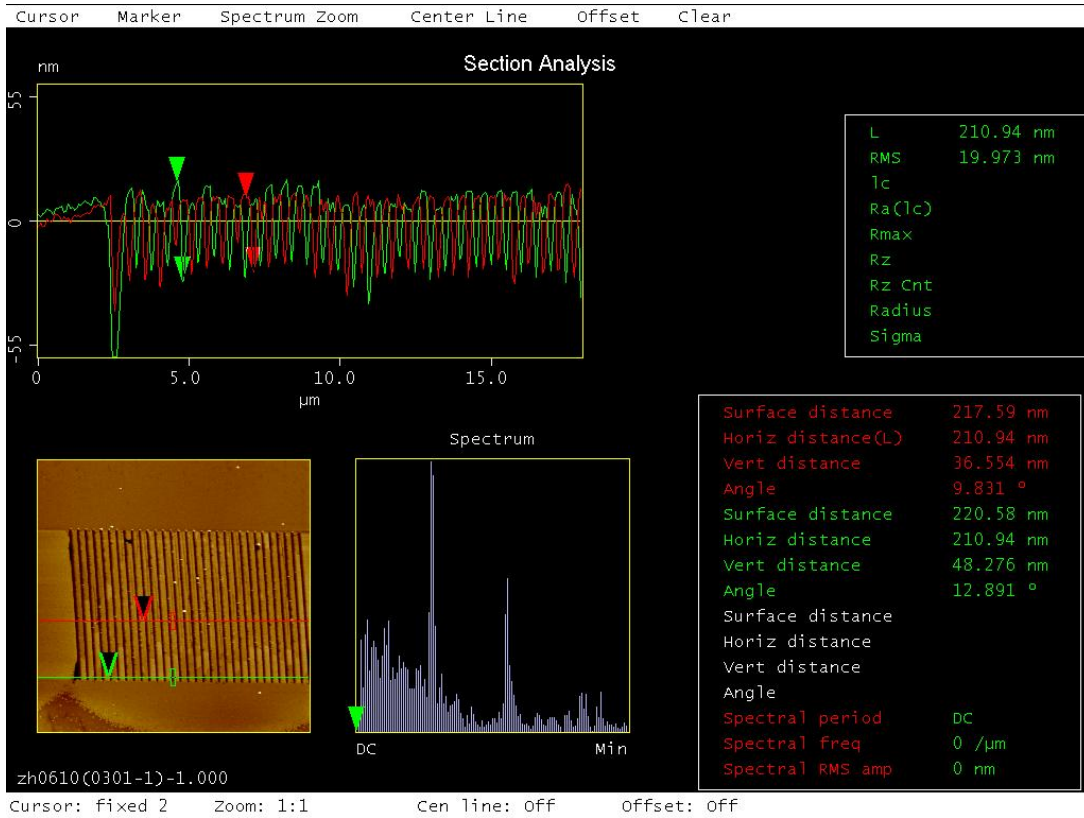


(c)
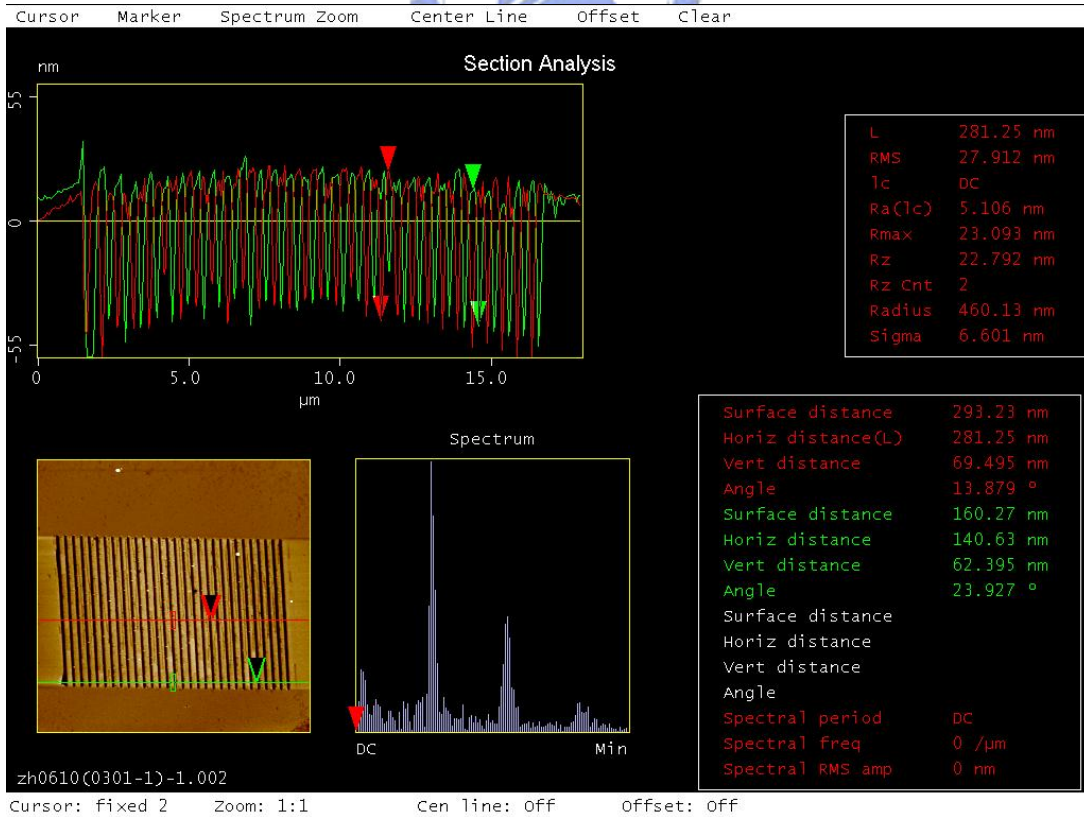
(d)
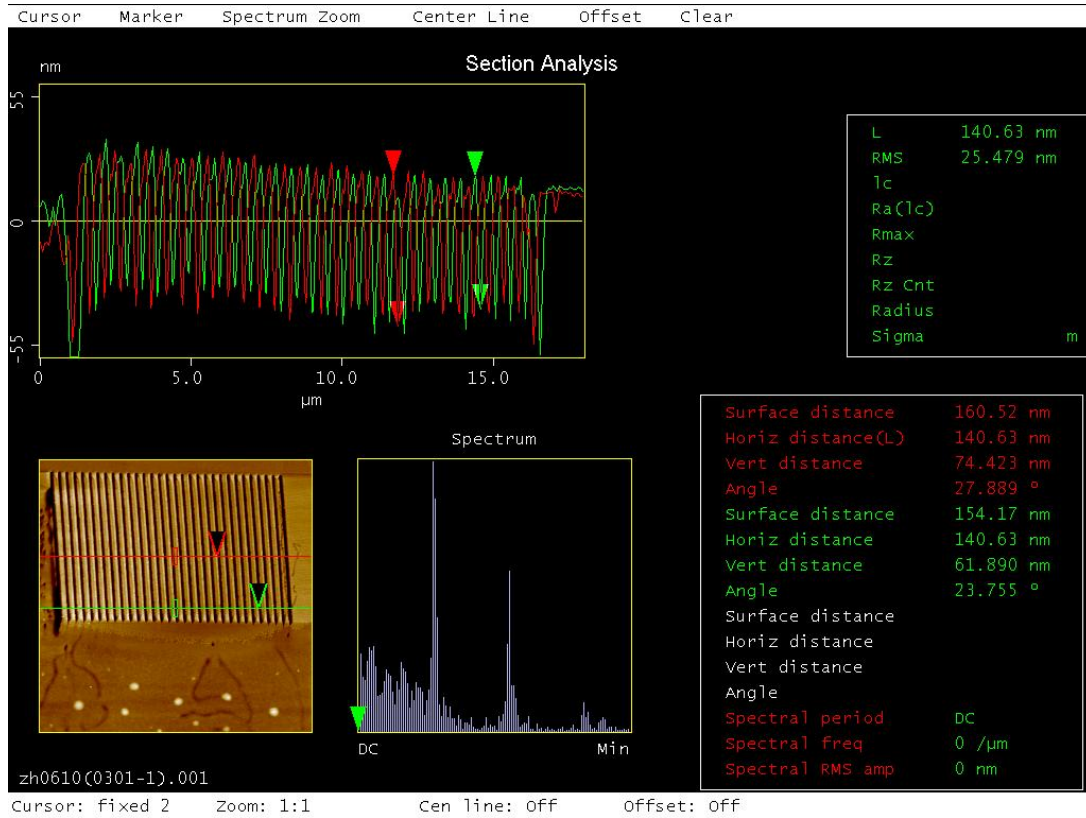


(e)
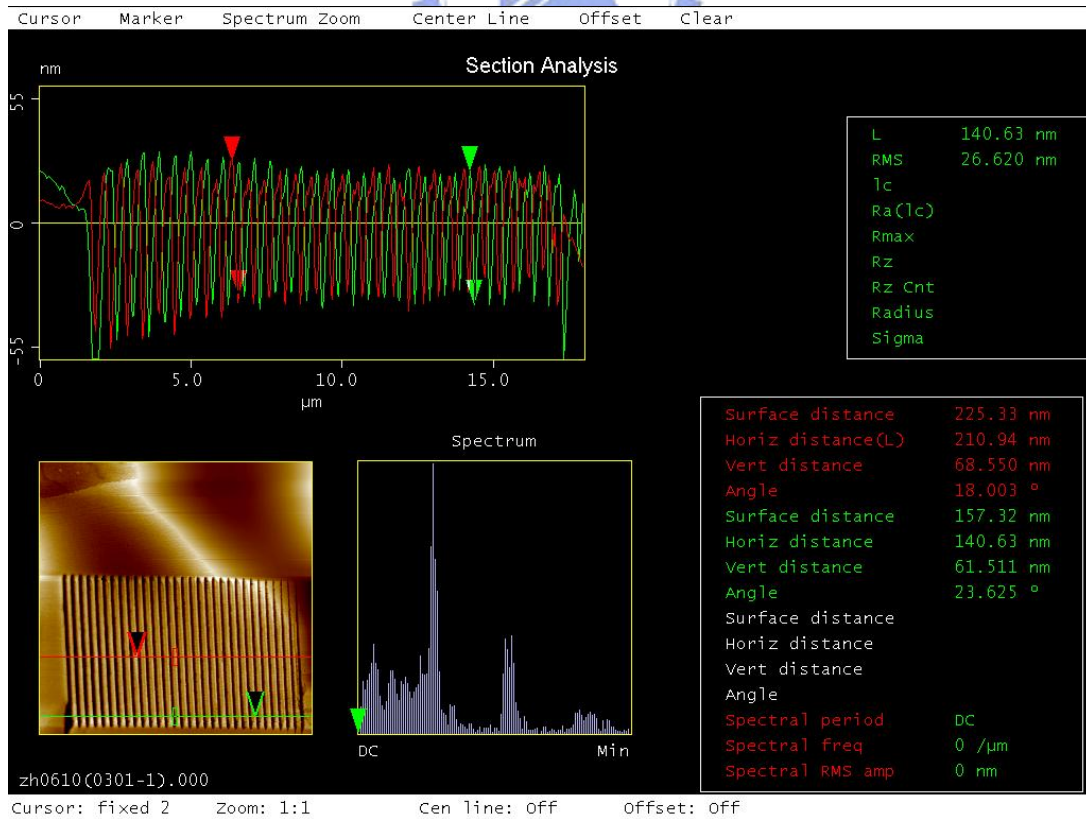
(f)
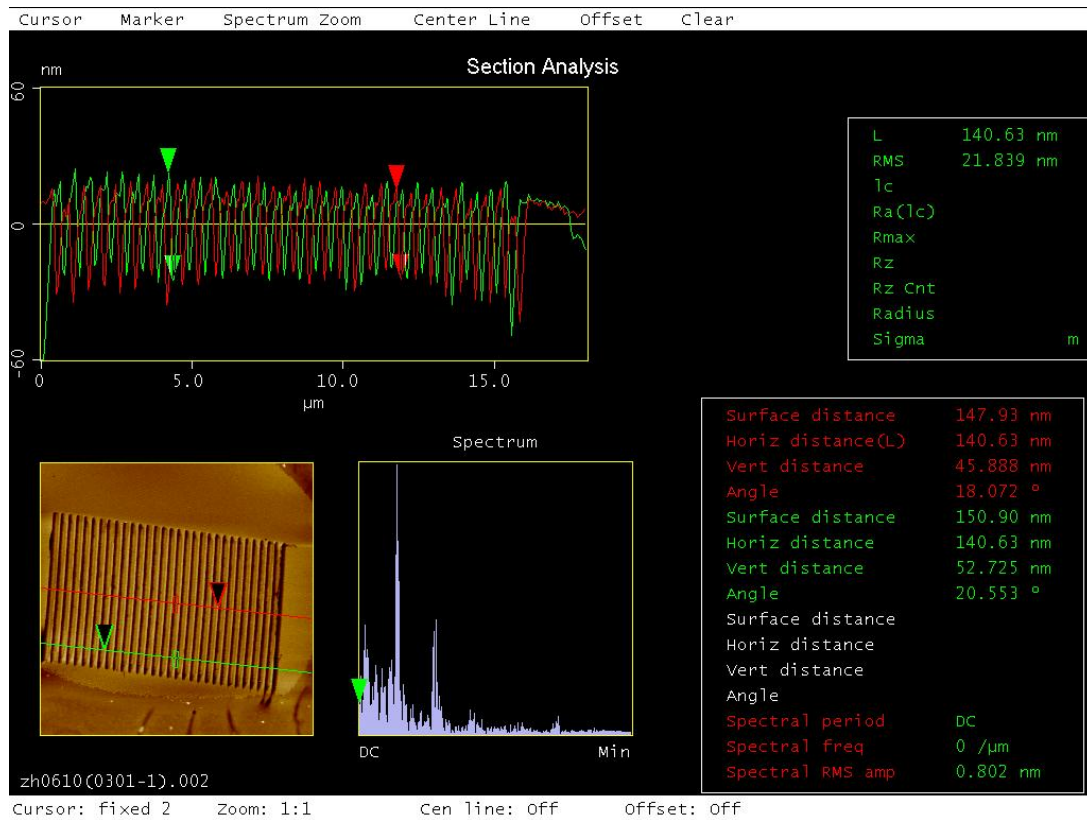


(3)
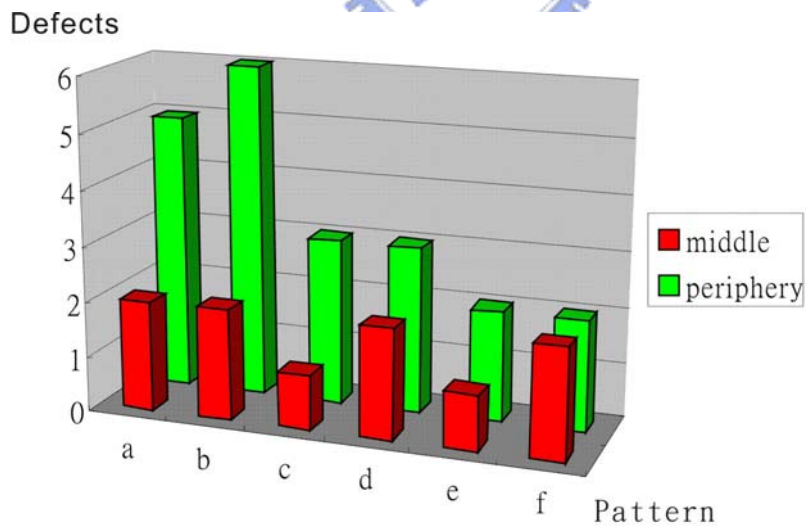


Fig. 40 (1)The illustration shows the layout of the imprint result , the red frame
represents the mold imprinting area (2) (a)~(f) represents the imprint result in
different place (3) the simple calculation of the defects in the middle and
periphery of the nano-grating patterns

Table 1 Comparison of advantages and disadvantages of anti-sticking
layers prepared by different methods[21]

| Method | Advantage | Disadvantage |
|---|---|---|
| Spin coating | 1.Easy to fabricate<br>2.Thick film formation<br>  High reproducibility and reliability<br>3.Well-known and traditional method | 1.Hard to make below a 100 nm thickness<br>2.Hard to make a uniform coating on patterned surfaces<br>3.Can waste up to 98% of process materials |
| Liquid SAM | 1.Relatively cheap process<br>2.Strong chemical bonding | 1.Insufficient wetting for nano-structures<br>2.Low reproducibility and reliability in a large area<br>3.Waste of organic chemicals<br>4.Substrates dependant |
| Vapor SAM | 1.Easier to fabricate than liquid process<br>2.High reproducibility and high reliability | 1.Relatively higher temp.<br>2.No control of film thickness<br>3.Substrates dependant |
| Plasma polymerization | 1.Low temperature process<br>2.Thickness control from nanometer to micrometer at any substrate<br>3.High reproducibility and high reliability<br>4.Substrates independent<br>5.Semiconductor process compatible | 1.Relatively expensive<br>2.Relatively weak physical bonding |

Table 2 The overall parameters of imprint process by our home-made
nanoimprintor

| | H-NIL | UV-NIL | | FIS |
|---|---|---|---|---|
| Mold | Si | ITO glass | | Si |
| Process | Lift-off、RIE | Lift-off | | × |
| Resist | PMMA 495k | PAK-01 -60 | SU-8 2000.5 | PMMA 459k |
| Spin speed(rpm) | 4000~5000 | 3000~6000 | 3000~4000 | 1000~5000 |
| Bubble density after spin coat | Low | High | Low | Low |
| Prebake tem. | 100℃ | × | 95℃ | 100℃ |
| Prebake time | 1 min | × | 2 min | 1 min |
| thickness(nm) | 170~130 | 80~70 | 120~80 | 300~130 |
| Imprint tem. | 120-160℃ | RT | RT | 120-160℃ |
| Imprint time | 7 min | 5 min | 5 min | 7 min |
| Exposure time | × | 10 min | 10 min | × |
| PEB tem. | × | × | 95℃ | × |
| Preimprint force | 0.1MPa | 0.1MPa | 0.1MPa | 0.1MPa |
| Imprint force | 0.4MPa | 0.6MPa | 0.6MPa | 0.4MPa |
| Mold size | ~ 4cm$^2$ | 2 cm$^2$ | 2 cm$^2$ | ~ 4cm$^2$ |
| Base pressure | 50 mtorr↓ | 50 mtorr↓ | 50 mtorr↓ | 50 mtorr↓ |
| ASL | BA-m | × | DDTS | × |

Table 3. The classification and parameters of different types of solar cell

| Classification[a] | Effic[b] (%) | Area[c] (cm2) | $V_{oc}$ (V) | $J_{sc}$ (mA/cm2) | FF[d] (%) |
|---|---|---|---|---|---|
| **Silicon** | | | | | |
| Si (crystalline) | 24.7±0.5 | 4.00 (da) | 0.706 | 42.2 | 82.8 |
| Si (multicrystalline) | 20.3±0.5 | 1.002 (ap) | 0.664 | 37.7 | 80.9 |
| Si (thin film transfer) | 16.6±0.4 | 4.017 (ap) | 0.645 | 32.8 | 78.2 |
| Si (thin film submodule) | 9.4±0.3 | 94.9 (ap) | 0.493[f] | 26.0[f] | 73.1 |
| **Ⅲ-Ⅴ Cells** | | | | | |
| GaAs (crystalline) | 25.1±0.8 | 3.91 (t) | 1.022 | 28.2 | 87.1 |
| GaAs (thin film) | 24.5±0.5 | 1.002 (t) | 1.029 | 28.8 | 82.5 |
| GaAs (multicrystalline) | 18.2±0.5 | 4.011 (t) | 0.994 | 23.0 | 79.7 |
| InP (crystalline) | 21.9±0.7 | 4.02 (t) | 0.878 | 29.3 | 85.4 |
| **Thin Film Chalcogenide** | | | | | |
| CIGS (cell) | 18.4±0.5[g] | 1.04 (ap) | 0.669 | 35.7 | 77.0 |
| CIGS (submodule) | 16.6±0.4 | 16.0 (ap) | 0.661[f] | 33.4[f] | 75.1 |
| CdTe (cell) | 16.5±0.5[g] | 1.032 (ap) | 0.845 | 25.9 | 75.5 |
| **Amorphous/Nanocrystalline Si** | | | | | |
| Si (amorphous)[h] | 9.5±0.3 | 1.070 (ap) | 0.859 | 17.5 | 63.0 |
| Si (nanocrystalline) | 10.1±0.2 | 1.199 (ap) | 0.539 | 24.4 | 76.6 |
| **Photochemical** | | | | | |
| Dye sensitised | 10.4±0.3 | 1.004 (ap) | 0.729 | 21.8 | 65.2 |
| Dye sensitised (submodule) | 6.3±0.2 | 26.5 (ap) | 6.145 | 1.70 | 60.4 |
| **Organic** | | | | | |
| Organic polymer[i] | 3.0±0.1 | 1.001 (ap) | 0.538 | 9.68 | 52.4 |
| **Multijunction Devices** | | | | | |
| GaInP/GaAs/Ge | 32.0±1.5 | 3.989 | 2.622 | 14.37 | 85.0 |
| GaInP/GaAs | 30.3 | 4.0 (t) | 2.488 | 14.22 | 85.6 |
| GaAs/CIS (thin film) | 25.8±1.3 | 4.00 (t) | — | — | — |
| a-Si/mc-Si (thin submodule)[j] | 11.7_0.4 | 14.23 (ap) | 5.462 | 2.99 | 71.3 |

**a.** CIGS=CuInGaSe2；a-Si = morphous silicon/hydrogen alloy. **b.** Effic = efficiency. **c.** (ap) = aperture area；(t)=total area；(da) = designated illumination area. **d.** FF = fill factor. **e.** FhG-ISE = Fraunhofer Institut fur Solare Energiesysteme；JQA = japan Quality Assurance；AIST = Japanese National Institute of Advanced Industrial Science and Technology. **f.** Reported on a "per cell" basis. **g.** Not measured at an external laboratory.

**h.** Stabilized by 800 hours , 1 sun AM1.5 illumination at a cell temperature of 50℃. **i.** Stability not investigated.

**J.** Stabilized by 174 hours, 1 sun illumination after 20 hours, 5 sun illumination at a sample temperature of 50℃.

# Reference

[1] http://www.itrs.net/

[2] http://www.sematech.org/

[3] Stephen Y. Chou, Peter R.krauss, Preston J. Rrnstrom, Appl. Phys. Lett. Vol.67(21), pp3114-3116, 1995

[4] M. Bender, M. Otto, B. Hadam, B. Spangenberg, and H. Kurz, Microelectronic Engineering Vol.53, pp.233–236, 2000

[5] Y. Xia, G. M. Whitesides, Angew. Chem. Int. Vol.37, pp.550-575, 1998

[6] Lingjie Guo, Peter R. Krauss, and Stephen Y. Chou , Appl. Phys. Lett. Vol.71(13), pp.1881-1883, 1997

[7] A. Pe´pin, P. Youinou, V. Studer, A. Lebib, Y. Chen , Microelectronic Engineering, Vol. 61–62,pp.927–932, 2002.

[8] Mingtao Li, Hua Tan, Lei Chen, Jian Wang, and Stephen Y. Chou, J. Vac. Sci. Technol. B Vol.21, pp.660-663, 2003

[9] Y. H. Cho, S.W. Lee, B. J. Kim and T. Fujii, Nanotechnology,Vol. 18,pp.465303, 2007

[10] M. Colburn, et al., "Step-and-flash Imprint Lithography: A New Approach to High Resolution Patterning," *Proc. of SPIE*, Vol.3676, pp.379, 1999.

[11] Y. Xia, G. M. Whitesides, Angew. Chem. Int. Vol.37, pp.550-575, 1998

[12] Stephen Y. Chou Chris Keimel & Jian Gu, Nature Vol.417, pp835 - 837, 2002

[13] Xiaogan Liang , Wei Zhang, Mingtao Li, Qiangfei Xia, Wei Wu,

Haixiong Ge, Xinyu Huang, Stephen Y. Chou, Nano Letters Vol.5, No.3, pp527-530, 2005

[14] N Chaix, C Gourgon, S Landis, C Perret, M Fink, F Reuther and D Mecerreyes, Nanotechnology Vol.17, pp4082–4087, 2006

[15] Nanonex Corporation, Monmouth Junction, NJ, USA 08552

[16] M. Bender, M. Otto, B. Hadam, B. Spangenberg, and H. Kurz, Microelectronic Engineering Vol.53, pp.233–236, 2000

[17] Leonard F. Pease III, Paru Deshpande, Ying Wang, William B. Russel and Stephen Y. Chou, Nature Nanotechnology Vol. 2, pp545-548, 2007

[18] Nicholas A. Melosh, Akram Boukai, Frederic Diana, Brian Gerardot, Antonio Badolato, Pierre M. Petroff, James R. Heath, Nature Vol.300, pp112-115, 2003

[19] James R. Heath, Nicholas A. Melosh , Akram Boukai, Science 300, pp.112-115, 2003

[20] Jinan Chai, Dong Wang, Xiangning Fan And Jillian M. Buriak, Nature Nanotechnology Vol.2, pp500-506, 2007

[21] Ahmed Busnaina,2007, ''Nanomanufacturing Handbook'' , CRC Press/Taylor & Francis, Boca Raton

[22] Nils ROOS', Thomas Luxbacher'', Thomas Glinsner'', Karl Pfeiffef, Hubert Schu1z', Hella-C. Scheer, Proceedings of SPIE, Vol 4343, pp.427-435, 2001

[23] Zhaoning Yu,He Gao, Wei Wu, Haixiong Ge, and Stephen Y. Chou, J. Vac. Sci. Technol. B, Vol. 21(6), pp.2874-2876, 2003

[24] Lei Chen, Jian Jim Wang, Frank Walters, Xuegong Deng, Mike Buonanno, Stephen Tai, and Xiaoming Liu, Appl. Phys. Lett. , Vol.

**90**, pp. 063111, 2007

[25] Seh-Won Ahn, Ki-Dong Lee, Do-Hwan Kim, and Sang-Shin Lee,

Ieee Photonics Technology Letters, Vol.17, pp.2122-2124, 2005